Original article

Brain targeting stealth lipomers of combined antiepileptic-anti-inflammatory drugs as alternative therapy for conventional anti-Parkinson's

Iman M. Higazy

Department of Pharmaceutical Technology, National Research Center, 33 Albohouth St., Dokki, Cairo, Egypt

ABSTRACT

This study presents an alternative therapy to conventional anti-Parkinson's treatment strategies; where motor and non-motor symptomatic complications are considered. Thus; providing sustainability, patient compliance, therapeutic safety and efficiency, based on triggering secretion of endogenous dopamine (DA). Exogenous DA has long been considered the best therapy, however, its poor blood brain barrier (BBB) permeability, fluctuated plasma levels, and non-motor complications negligence, decreased response to therapy with time. Consequently; brain targeting Tween®80-coated pegylated lipomers were tailored for intravenous administration (IV) of L-Dopa, and two drugs of reported neuroprotective effect: lamotrigine (LTG) and tenoxicam (TX). Single-step nanoprecipitation method was used; for its reproducibility and ease of scaling-up. Formulation targeting and anti-PD efficiency was evaluated against marketed standards and L-Dopa. In-vitro and in-vivo pharmacokinetic and dynamic studies were carried out for setting optimization standards upon varying inter-components ratio. Results revealed that lipomers are, generally, significantly efficient in brain targeting compared to oral tablets. LTG-lipomers (LF20) showed the maximum anti-PD compared to its TX and L-Dopa analogues. Combining LTG and TX had synergistic effect; highlighting a new prescription for both drugs. Thus; offering a safe, targeted, and therapeutically efficient sustained dosage form, capable of mitigating PD risk and treating it though weekly administration. Hence; presenting a novel promising anti-neurodegenerative strategy; on employing various mechanisms that were previously achieved through additional therapeutic supplements.

© 2019 The Author(s). Published by Elsevier B.V. on behalf of King Saud University. This is an open access article under the CC BY-NC-ND license (http://creativecommons.org/licenses/by-nc-nd/4.0/).

1. Introduction

Parkinson's (PD) is a progressive motor disease, globally propagating with no gender preference, expressed through a series of neuropathic features including degeneration of dopaminergic neurons in substantia nigra (SN) of mid-brain, and neuro-inflammation; resulting in cardinal motor symptoms as tremors, rigidity, bradykinesia, poor balance, and difficulty in walking, in addition to other non-motor symptoms resulting from autonomic nervous system dysfunction including hallucination, psychiatric and cognitive impairment (Chaudhuri et al., 2011). Generally;

pharmacologic strategy for PD treatment is based on exogenous DA. This is a natural neurotransmitter and neurohormone, exerting critical role in various body systems, including CNS, circulatory, renal, as well as, digestive and immune systems (Senek and Nyholm, 2014), however, it cannot be directly administered due to its hydrophilic nature hindering its brain blood barrier (BBB) penetration. Thus; DA replacement therapy was considered, including several DA receptor agonists, cholinesterase inhibitors, antimuscarinic drugs, MAO-B inhibitors and DA precursors as L-Dopa. However; these barely lead to partial recovery, since they particularly focus on improving motor symptoms only (Schapira, 2009).

Sinemet® is one of the most widely used anti-Parkinson's drug, comprising L-Dopa (LD) and carbidopa. The former is a direct DA precursor, facilitating its delivery across the BBB, while the latter decreases the peripheral breakdown of LD though decarboxylase inhibition (Olanow et al., 2009). Although, LD is highly efficient in early stage treatment of PD, nevertheless, on chronic long-

term treatment, motor complications; on–off phenomenon and dyskinesia, are usually reported in patients; due to excess dopaminergic tone (Porras et al., 2014). Moreover, its oral administration has low bioavailability; with only 1 to 10% LD reaching the CNS, due to its erratic gastrointestinal metabolism prior to its active transport though duodenum into the bloodstream, resulting in fluctuated cranial DA levels, in addition to a number of systemic side effects, as cardiac arrhythmias, hypotension and vomiting. As a result, various strategies were employed to ensure constant DA levels in brain, focusing on inhibition of peripheral LD breakdown, and its immediate release from formulations to shorten its circulatory biological half-life (1–3 h), which can be prolonged, later on, though catechol-O-methyl transferase (COMT) or dopa-decarboxylase (DDC) inhibition (Brooks, 2008).

Neuroinflammation is one of the key features of PD pathogenesis; that is thought to contribute to cell death in patient's brain. It is attributed to activation of microglia in SN; resulting from increasing pro-inflammatory cytokines in cerebrospinal fluid and basal ganglia together with aggregated nitrated forms of toxic α-synuclein (Mcgeer and Mcgeer, 2007). Non-steroidal anti-inflammatory drugs (NSAIDs) are immuno-modulating and anti-inflammatory agents; acting though inhibition of pro-inflammatory cyclooxygenase (COX) enzymes, providing neuro-protection against degeneration, reactive oxidative species and glutamate induced toxicity by inhibiting the activation of nuclear factor-kB; which have all been implicated in PD pathogenesis (Teismann and Ferger, 2001). However; the exact dose that would provide ideal neuroprotection, is still controversial, although regular administration of NSAIDs proved clinically efficient as per previous clinical trials reporting a consequent 45% decline in PD risk (Chen et al., 2003).

Tenoxicam (TX) is a NSAID with an anti-oxidant, neuroprotective anti-PD effect; proved though several epidemiologic evidences linking neuroinflammation and PD risk. Its mode of action is based on inhibition of nitric oxide radicals generating system, and modulation of transcription factors related to inflammatory reactions including cytokine expression; associated with PD neurodegenerative pathogenesis, as per several previous studies linking that inflammatory gene cytokine polymorphisms of TNF-α and IL1-β to the increase in PD risk (Bassani et al., 2015).

Excitotoxicity is another key pathogenic mechanism of PD attributed to glutamate; whose receptors are abundant in dopaminergic neurons of SN, inducing cell death though N-methyl-D-aspartate (NMDA) receptor activation. However; NMDA receptor antagonists, although neuroprotective, they have limited use due to their low potency and tolerability (Jankovic and Hunter, 2002), hence; a promising glutamate antagonist is needed. Furthermore; free radicals play crucial role in inducing PD. Although several therapeutics as monoamine oxidase B (MAO-B) inhibitors, coenzyme Q10, and creatine have reported neuroprotective effects, none has proved promising in mitigating PD pathogenesis or even slowing its progression. Non-dopaminergic pharmacotherapy represented though adenosine receptor antagonists, as L-Dopa, although specifically efficient against PD motor fluctuations, still, they do not provide efficient final treatment to PD, due to lacking effect on non-motor symptoms (Hampel et al., 2017).

Lamotrigine (LTG) is a phenyl-triazine antiepileptic drug, whose neuroprotective properties have been efficiently demonstrated on improving histological and behavioral deficits accompanying brain damage in various cellular and experimental animal models. It is believed to act on stabilization of the presynaptic membrane, thought reducing its neuronal depolarization, and glutamate release at the excitatory synapse (Leng et al., 2013). This occurs though a number of putative molecular mechanisms; involved in PD neurological pathophysiology. It acts though voltage-sensitive

sodium channels blockage and inhibition of high voltage-activated calcium currents interacting with the vesicular release of neurotransmitters. Blocking type II sodium channels occurs though selectively decreasing repeated natrium firings without disturbing the normal neuronal flow, thus; suppressing the post-synaptic release of excitatory amino acids (EAAs), repressing the pathological release and delivery of glutamate, leading to overall reduction in CNS excitability (Ahmad et al., 2018b).

Neuronal injury results from toxic action; partly attributed to oxidative stress exerted by the oxygen-derived free radicals, and strongly connected to excitotoxicity, resulting from the increased levels of EAAs as glutamate and other neurotransmitters contributing dominantly in cell damage and subsequent death. Such findings perceives EAAs reduction as the main mode of neuroprotective action of LTG (Papazisis et al., 2008). Furthermore; LTG would modulate neurotransmission via interference with glutamatergic neurotransmission involving NMDA receptors; manifesting its anti-inflammatory properties, attributed to reduction in NMDA-mediated arachidonic acid (AA) signaling in brain (Kim et al., 2011).

Lipomers are lipid-polymer hybrid nanoparticles combining characteristics of both liposomes and polymeric nanoparticles, forming a unique drug delivery platform with high potential for differential targeting of cells or tissues, in addition to its biocompatibility, biodegradability, high structural integrity, excellent encapsulation efficiency, safety and controlled drug release. However, a major barrier for its effective delivery of various drugs to the target site is their sequestration by cells of the mononuclear phagocytic system (MPS), and then quick elimination from systemic circulation (Gajra et al., 2015). With consideration to data presented, using non-ionic surfactants as NPs coating enables non-invasive brain delivery of agents, including low molecular drugs, macromolecules, and other biological entities, that cannot independently permeate BBB in therapeutically effective concentrations. Binding to the particles also may offer clinical advantages such as decreased drug dose, reduced drug side effects, increased drug viability, non-invasive routes of administration and improved patient quality of life. The nanoparticles may be especially helpful for the treatment of the disseminated and very aggressive brain tumor by fine-tuning polysorbate concentration but further clinical trials are required (Chacko et al., 2018).

The objective of this study is to develop Tween®80 coated lipomers for targeted brain delivery of L-Dopa and LTG/TX combined system, using FDA-approved components for safety considerations, for evaluating their targeting anti-PD efficiency against L-Dopa and corresponding oral standards. Nanoprecipitation technique was used for preparation, using adsorption for Tween®80 coating. Lipomer system is based on three distinct functional units: biodegradable hydrophobic polymeric core (Ester terminated PLCL 50:50), stealth hydrophilic shell, (PEG covalently conjugated to DSPE), for immune system recognition avoidance, systemic circulation half-life prolongation and stability enhancement, and finally, interfacial lipid monolayer at PLCL core/PEG shell interface, (Soya bean lecithin), acting as molecular fence against drug free diffusion out of NPs and water penetration rate reduction; promoting drug retention within the polymeric core, serum stability and drug release sustainability (Zhang et al., 2008).

2. Materials

Lamotrigine was kindly donated by Delta Pharma, Egypt, Lamictal® conventional tablets, GlaxcoSmithKline Inc., USA. Tenoxicam was kindly donated by EIPICO Pharma, Egypt, Epicotil® conventional tablets, EIPICO Pharma, Egypt. L-Dopa was kindly donated by Egyphar, Egypt. Sinemet® tablets, Merck, Egypt. Ester termi-

nated poly (d, l-lactide-co-caprolactone) PLCL (50:50) of IV 0.79, was purchased from Lactel Bioabsorbables, USA. Lecithin; Soybean phosphatidylcholine (SPC, LipoidVR S100) was kindly supplied by Lipoid GmbH, Ludwigshafen am Rhein, Germany. Acetone for HPLC, ethyl acetate, sodium azide, sodium hydroxide and potassium dihydrogen orthophosphate were purchased from Sisco Research Laboratories, Mumbai, India. Sodium phosphate dibasic heptahydrate was purchased from Riedel-de Haën, Germany. Ethanol absolute HPLC grade, trichloroacetic acid solution, and Methanol (HPLC grade) were purchased from Fluka (Buchs, Switzerland). Polyethylene glycol (PEG) covalently conjugated by carboxylic acid to (DSPE): 1,2-distearoyl-sn-glycero-3-phosphoethanolamine-N-[carboxy(polyethylene- glycol)-2000], were purchased from Avanti Polar Lipids (Alabaster, AL). Acetonitrile HPLC Grade was purchased from Ranbaxy Fine Chemicals Ltd., Mumbai. Ultra-4 centrifugal Millipore filter (molecular weight cut-off of 10,000 Da), and 0.45 and 0.22 μm ISOPORE™ membrane filters, were purchased from EMD Millipore®, Ireland. Dialysis tubing cellulose membrane (molecular weight cut off 12,000 g/mole), Thiobarbituric acid/Trichloroacetic acid (TBA–TCA) reagent, Chlorpromazine hydrochloride, Griess reagent, hydrogen peroxide, 5,5′-dithiobis-(2-nitrobenzoic acid) reagent, Bovine serum albumin (BSA), and Tween®80 were purchased from Sigma–Aldrich, Germany. Carbidopa was purchased from the United States Pharmacopeia (Rockville, MD, USA). Human plasma (BioChemMed, Winchester, VA). Dulbecco's minimum essential medium (DMEM), Fetal bovine serum (FBS), Gentamycine, and L-glutamine were purchased from Invitrogen Life technologies, Argentina. All other analytical grade chemicals were used during experiment.

3. Methods

3.1. Preparation of stealth lipomers

Stealth lipomers were prepared by single-step nanoprecipitation method, as follows: 25 mg drug was dissolved in 5 ml ethanol, then mixed with 20 ml acetone/PLCL solution with polymer concentration of 5 mg/ml. Lecithin/PEG mixture of weight ratio 8.5:1.5, and total weight ratio to PLCL of 15%, were dissolved in 5%w/v ethanol absolute, then heated to 65 °C for complete lipid solubilization. The prepared PLCL/drug solution was then added to the lipid solution drop wisely under gentle stirring on magnetic stirrer (Wisestir® digital hotplate magnetic stirrer MSH-30D, PMI-Labortechnik Gmbh, Germany) at 150 rpm, then vortexed vigorously (Paramix II vortex, Julabo Labortechnik Gmbh, Germany) for 3 min followed by gentle stirring for 2 h at room temperature. The solution was then washed three times using Ultra-4 centrifugal Millipore filter to remove excess organic solvent (Chen et al., 2011). Then 20 ml of 1%w/v polysorbate 80 solution was added drop wisely, under constant stirring for 4 h, to the condensed solvent-free lipomer suspension, to be centrifuged at 24,000 rpm (Table top cooling ultracentrifuge, Sigma 3-30KS, Sigma Laborzentrifugen GmbH, Germany) for 30 min at −4 °C, then lyophilized (Josephine et al., 2014) (Lyophilizer, FD-81, Eyela, Japan). Blank PEG–lipid–PLCL NPs were also prepared by the same procedure.

3.2. Characterization of nanoparticles

3.2.1. Nanoparticle morphology characterization

Surface morphology of optimized HNPs was determined using transmission electron microscopy (JEOL, JEM-1230 transmission electron microscope, Japan). Approximately 1 ml of HNPs dispersion was dropped on a 300 mesh copper grid coated with carbon film and allowed to air-dry for 10 min, to be then stained with 2% w/v phosphotungstic acid solution with several replications and dried at room temperature. Digital micrograph and Soft Imaging Viewer software were used to perform the image capture and analysis (Ahmad et al., 2018a).

3.2.2. Particle size (PS), polydispersity index (PDI) and zeta potential (ZP)

Average particle size, polydispersity index (PDI) and zeta potential were measured by dynamic light scattering technique (Zetasizer, Malvern Instruments, Malvern, UK), at 25 °C and scattering angle 90°, with all measures in thrice. Average PDI and ZP were indicative of particle homogeneity, maximum repulsion force and consequent long term stability (Ahmad, 2017).

3.2.3. Drug loading (DL) and entrapment efficiency (EE)

A fixed quantity of HNPs dispersions; about 10 ml, was fractionated at 24,000 rpm for 30 min at 20 °C (Table top cooling ultracentrifuge, Sigma 3–30 KS, Sigma Laborzentrifugen GmbH, Germany), where the supernatant fraction was analyzed spectrophotometrically at the corresponding λ_{max} of each drug (Shimadzu 1800, Japan) for determination of unencapsulated drug. The drug loading (%) and entrapment efficiency (%) were calculated using the following equations (Kumar et al., 2013):

$$DL\,(\%) = [(W_t - W_s)/(W_t - W_s + W_L)] \times 100 \qquad (1)$$

$$Drug\,EE(\%) = [(W_t - W_s)/(W_t)] \times 100 \qquad (2)$$

where; W_t is the total weight of drug used, W_s is the drug weight in supernatant after centrifugation and W_L is the weight of the lipid-polymer hybrid used.

3.2.4. In-vitro release study and kinetics

Dialysis bag diffusion technique was used as reported by Li et al. (2008), with modification; where the dialysis bag was primarily pre-soaked in warm PBS (phosphate buffer solution, pH 7.4) for 10 min (Sigma, Molecular weight cutoff 12,000), then an accurately weighed amount of HNPs containing 10 mg drug was transferred to each bag and sealed, to be suspended in a beaker containing 100 ml PBS and stirred at constant speed of 150 rpm at 37 °C using "Shaking incubator", GFL 3032, Germany. Aliquots of 2 ml were withdrawn at pre-set time points; and replaced by equal volume of fresh buffer. Mean cumulative percent of each drug released was spectrophotometrically analyzed in triplicate for each formulation (Ishak et al., 2017). Release data were kinetically analyzed using KineDS3 software, to be fitted with different kinetic models. This method was modified for the release studies of the corresponding conventional tablets of each drug type, as presented in the supporting documents

3.2.5. In-vitro stability

A 1 mg/ml solution of each of the selected lipomers, was separately incubated with: (a) 10%w/w BSA (bovine serum albumin) and (b) 10%w/w human plasma with heparin solution, at 37 °C under gentle stirring. At each time point for 2 h, an aliquot was collected to measure PS, as previously explained, in triplicate (Zhang et al., 2008), on considering PLCL/PEG and PLCL polymeric nanoparticles as controls.

3.2.6. In-vitro biocompatibility

3.2.6.1. Cell culture. Two types of cells were used: human cortical neuronal cells-2 (HCN2, American Type Culture Collection), and BBB hCMEC/D3cell-line (Merck KGaA, Darmstadt, Germany), as reference to human normal brain and BBB cells, respectively. Cells were maintained in DMEM supplemented with 10% FBS, 50 μg/mL gentamycine, and 2 mM L-glutamine, and cultured in 75 cm^2 culture flasks, kept at 37 °C in a humidified atmosphere of 5% CO2 (Zheng et al., 2007).

3.2.6.2. In-vitro biocompatibility "Cytotoxicity" assay. Cell viability was determined using the MTS assay (CellTiter 96® AQ$_{ueous}$ nonra-dioactive cell proliferation assay, Promega, Wisconsin, USA); with cells seeded in a 96-well plates (Corning Costar, Fisher Scientific, USA) at a density of 10,000 cells/well. After 24 h, 5 ul of lipomer dispersions were added in 200 ul of medium to be incubated at 37 °C for 48 h in a humidified 5% CO_2 atmosphere. Then medium was replaced for fresh one, and cells were allowed to equilibrate for 1 h, then 20 μl/well of MTS reagent (combined MTS/PMS solution) were added and manipulated according to the manufacturer's instructions (Vega-Avila and Pugsley, 2011), followed by quantification of optical density (OD) at 490 nm using an ELISA plate reader. Values were expressed in terms of percent of untreated control cells set as 100% and viability was determined as percentage of the OD from control cells (Bãnez-Coronel et al., 2008), where each point represents the mean ± SD of four replicates for each treatment.

3.2.7. In-vivo pharmacokinetic studies

3.2.7.1. Experiment design. Protocol of studying brain targeting efficiency of formulations was approved by Ethics Committee of National Research Center, Egypt. Seven groups of male albino Wistar rats (adult/weighing 200–250 g), each comprising six rats were housed in polypropylene cages and kept under standard laboratory conditions; room temperature and 40–70% relative humidity on receiving treatment as follows: Group 1 (Lamictal® conventional tablets), Group 2 (IV selected LTG lipomers), Group 3 (Epicotil® conventional tablets), Group 4 (IV selected TX lipomers), Group 5 (Sinemet® conventional tablets), Group 6 (IV selected L-Dopa lipomers), and Group 7 (Control group subdivided into 7a: receiving IV placebo lipomers and 7b: receiving oral placebo).

As per Ammar et al. (2018), dose was calculated based on "rat body weight: surface area" ratio. At pre-determined time intervals, rats were anesthetized with chloroform and decapitated, with skulls cut opened. Brain was removed, rinsed twice with normal saline to remove adhering tissue/fluid, weighed and homogenized using glass homogenizer in an ice-cold bath, with 5 ml/g physiological PBS pH 7.4, then transferred into clean sterile tubes. Blood samples were collected from the trunk; in heparinized tubes by *retro*-orbital puncture, then centrifuged at 3,000 rpm for 15 min. Supernatant was collected and transferred into clean sterile tubes. Homogenized brain and separated plasma tubes were stored at −80 °C. Process calibration and assay validation were also carried out, with detailed results attached in the supporting documents.

3.2.7.2. Processing blood and brain tissue for HPLC analysis. Based on method presented by Castel-Branco et al. (2001) and Sallustio and Morris (1997): Aliquot of 1 ml plasma was added to 1 ml 2 N NaOH solution, then added to 5 ml ethyl acetate (HPLC grade Mwt. 88.10 Da), and vortexed for 1 min at 500 rpm, and centrifuged for 10 min at 10,000 rpm. The upper organic layer was transferred to clean glass tube and allowed to evaporate to dryness at 45 °C using nitrogen evaporator. Residues were reconstituted in 1 ml IS (10μg/ml) solution dissolved in 100 μl mobile phase, and vortexed for a minute at 500 rpm, to be finally injected into HPLC system. For brain homogenate; 1 ml was inserted into glass tube, with 100 μl of 20% trichloroacetic acid solution added for deproteinization, and centrifuged at 3000 rpm for 15 min at 15 °C. Supernatant was transferred to 10 ml tube and submitted to liquid–liquid extraction into ethyl acetate after basification, as described for plasma. Standard and control samples were similarly prepared. All results were processed according to WinNonlin® software (Pharsight Co., Mountain View, CA, USA).

3.2.8. In-vitro/in-vivo correlation

A point-to-point *in-vitro/in-vivo* correlation (IVIVC) for the selected lipomers was carried out for relating cumulative percentage of drug released *in-vitro* to its amount released in rat plasma and brain *in-vivo*; though employing correlation coefficient using the linear regression analysis.

3.2.9. In-vivo pharmacodynamic studies

3.2.9.1. Experimental design and dosing protocol. Healthy male albino wistar rats, 6–8 weeks old, weighing 200–250 g, were housed under standard laboratory conditions, and divided into 9 groups each comprising 8 rats: **Group 1- Positive control**; receiving placebo, **Group 2-Negative control**; receiving 3 mg/kg/day intrapretonial (i.p.) Chlorpromazine (CPZ) only. Groups 3, 4, and 5 are Standard group receiving CPZ i.p 3 mg/kg/day, followed by the oral dose administration (30 mg/kg) after 30 min on test day (Sandhu and Rana, 2013) as follows: **Group 3- Standard LTG** received Lamictal® tablet, **Group 4- Standard TX** received Epicotil® tablet, **Group 5- Standard L-Dopa** received Sinemet® tablet, Groups 6, 7, 8 and 9 are test groups received CPZ i.p 3 mg/kg/day, followed after 30 min by equivalent doses of IV lipomers on test day: **Group 6- LTG test** received I.V. LTG lipomer, **Group7- TX test** received I.V. TX lipomer, **Group 8- L-Dopa test** received I.V. L-Dopa lipomer, **Group 9-Combined** LTG/TX HNPs.

Pharmacodynamic evaluation was carried-out by following CPZ induced Parkinson's model for 21 days, where CPZ was administered in dose of 3 mg/kg/day i.p. Behavioral parameters; motor and cognitive, were investigated though: catalepsy, open field test, grip strength activity, water maze and passive avoidance tests (Shin and Chung, 2012). In addition; biochemical parameters were estimated through lipid peroxidation, nitrite levels, superoxide dismutase, reduced glutathione, and catalase assays (Vadlamudi et al., 2016), in a means of forming a complete pharmacodynamic profile for tested formulations. All experimental procedures involving animals were approved by National Research Center Animal Ethics Committee.

3.2.9.2. Behavioral assays.

3.2.9.2.1. Catalepsy. Catalepsy was performed at room temperature in calm conditions; without external interference. Severity of catalepsy (catalepsy score) was assessed using block test according to the following scoring system:

> <u>Step I</u>: After taking rats out of their cages, they were gently placed on a table and touched or pushed gently on the back. If the rat failed to retain his normal posture, then a score of 0.5 was to be assigned.
>
> <u>Step II</u>: On a 3 cm high block, the front paws of rats were placed alternately. If the rat failed to correct such posture within 15 s, a total score of 1 (0.5 for each paw), was to be added to the "step I" score.
>
> <u>Step III</u>: Again, the front paws of the rat were placed alternately, but this time on a 9 cm high block. If the rat failed to correct the posture within 15 s, a total score of 2 (1 for each paw), was added to scores of steps I and II. Thus, the highest total catalepsy score; cut-off score, cannot exceed 3.5 for each rat (Sharma et al., 2011).

3.2.9.2.2. Open field activity. Spontaneous locomotor activity of rats was assessed using a white plywood board measuring 72 cm length × 36 cm height × 72 cm width, uniformly divided into equal sized 16 squares; 18 cm × 18 cm each, that are lined for determination within an open arena enclosed within three black painted walls and forth wall of Plexiglas to be able to visualize the rats. For assuring results validity, rats' habituation to the arena

was carried out. On two consecutive days, each rat was independently placed into the central square, or one of the four corners of the open field and allowed to explore the arena for 5 min, after which, they were returned to cages. On the experiment day, rats were kept in the central square for 10 min, to provide sufficient surrounding space for rats of high locomotor activity that might cross the field lines more than once. Test and standard drugs were administered on the 21st day and activity was recorded 15 min later. Number of squares/lines crossed was counted to calculate total distance crossed by rats in the arena (Sestakova et al., 2013).

3.2.9.2.3. Grip strength. Wire hanging test was applied, using an apparatus comprising a stainless steel bar with two platforms, under the condition of briefly training rats before the test session, represented though placing each rat separately on the stainless steel bar, allowing it to grip the bar. Grip strength and muscular tone were observed and evaluated though a time-based scoring system with cut-off time of 300 s; representing the maximum length of time a rat would manage to hold the bar before it fell again (Takahashi et al., 2009).

3.2.9.2.4. Water maze test. To assess spatial learning behavior of rats, a 12 cm deep "water maze" composed of a 60×30 cm rectangular transparent Plexiglas tank filled with water, maintained at room temperature and made opaque by dissolving starch in it, up to 2 cm above a 15×13 cm fixed Plexiglas platform surface. Before the test session, rats were trained in the maze for habituation, then each was individually placed in water, facing the tank wall; where it was allowed to stay for 10secs to locate and climb onto the submerged platform. Note that rats should be guided, if they failed to find the platform within the allowed time. Memory was evaluated by recording "retention latency"; time, in seconds, taken by a rat to reach the platform, where cutoff time not exceeding 2 min. Readings were recorded 1 h (short term memory) and 24hs (long term memory) after the habituation session (Vorhees and Williams, 2006).

3.2.9.2.5. Passive avoidance test. To assess fear aggravated learning and memory behavior in rats, "passive avoidance apparatus" with grid floor and steel bars was used. It is divided into two compartments; one of which is non-illuminated (punishable box); where rats receive a 1.5 mA foot shock for five seconds when they reach it, while the other is bulb illuminated (safe box). Rats are left to move freely between both compartments though the sliding door separating them. Once the foot shock is received, rata are expected to rapidly leave to the safe box. Rats were trained 24 h before test session for habituation, and an hour before experimentation, standard and test drugs were administered and latency time was noted as numerical indicator (Li et al., 2013).

3.2.9.3. Biochemical assays.
3.2.9.3.1. Lipid peroxidation. Lipid peroxidation was estimated colorimetrically in brain tissue by quantifying TBARS according to the method of Niehaus and Samuelson (1968). Animals were sacrificed by cervical dislocation and the brain was dissected out and washed in ice-cold saline to remove any blood traces. Enzyme activity was assayed in 10%w/v brain homogenate prepared in 0.2 M of pH 8 phosphate buffer (Bishnoi et al., 2006), as per Wills method. Thiobarbituric acid reactive substances (TBARS) levels were estimated by treating the rat brain tissue homogenate with thiobarbituric acid–trichloroacetic acid (TBA–TCA) reagent. The homogenate mixture was heated for 15 min, then cooled and centrifuged for 10 min, and the colored supernatant was analyzed spectrophotometrically at 535 nm against blank reagent.

3.2.9.3.2. Reduced glutathione. was estimated following Ellman method (Ellman, 1959); where 1 ml of brain tissue homogenate was precipitated by addition of 1 ml of 10% TCA and centrifuged to collect the supernatant portion, of which 1 ml was treated with 0.5 ml of Ellman's reagent [5,50-dithiobis-(2-nitrobenzoic acid)]

and 3 ml PBS (0.2 M, pH 8.0), to be analyzed spectrophotometrically at 412 nm.

3.2.9.3.3. Catalase levels. was assayed colorimetrically at 620 nm and expressed as mM H_2O_2 (hydrogen peroxide) consumed per minute per mg protein; as per the method described by Sinha (1972); based on the principle of H_2O_2 decomposition by catalase enzyme evidenced with reduction of absorbance with time: A homogeneous mixture was prepared by combining 0.1 ml of brain tissue homogenate, 1.9 ml of 50 mmol/l PBS and 1 ml of 30 mmol/l hydrogen peroxide. Absorbance was noted down at 240 nm initially and after 3 min. The reaction was stopped by adding 2 ml dichromate-acetic acid reagent (5% potassium dichromate and glacial acetic acid mixed in ratio 1:3). Variation in absorbance values helps in estimating catalase levels (Radenovic et al., 2007).

3.2.9.3.4. Superoxide dismutase (SOD). **Superoxide dismutase (SOD)** determination was based on SOD mediated inhibition of nitro blue tetrazolium reduction to blue formazan by superoxide anions. Total protein in brain homogenate was estimated using an assay mixture comprising 0.1 ml brain homogenate, 1.2 ml sodium pyrophosphate buffer (pH 8.3, 0.052 M), 0.1 ml phenazine methosulphate (186 μM), 0.3 ml nitro blue tetrazolium (300 μM), and finally, 0.2 ml NADH (750 μM) for reaction initiation. This was kept at 30 °C for 90 s, then 0.1 ml glacial acetic acid was added to stop the reaction, followed by vigorous stirring with 4 ml n-butanol, then allowed to stand for 10 min, to be able to separate the n-butanol layer for determination of color intensity at 560 nm. The SOD activity was expressed in terms of nM/mg of total protein (TP) (Agarwal and Kale, 2001).

3.2.9.3.5. Nitrite levels. Nitrite levels were estimated from nitric oxide production using Griess reagent assay, based on the fact that increased oxidative-stress in brain leads to its damage producing nitric oxide, which would be oxidized spontaneously into nitrite and nitrate. Brain tissue homogenate and Griess reagent of equal volumes were incubated for 10 min and analyzed spectrophotometrically.

3.2.10. Statistical analysis

Results were expressed as mean ± SD (standard deviation) on applying ANOVA and *t*-test using SPSS 14.0 for Windows (SPSS Inc., USA) (Bence et al., 2003). Least Significant Difference (LSD) at 5% confidence level was set as level of significance.

4. Results and discussion

4.1. Preparation of stealth lipid/polymer hybrid nanoparticles

In contrast to other preparation techniques, this single-step self-assembly approach is favored for its cost-effectiveness and scalability, while would guarantee a high yield with minimum production time and batch-to-batch variation (Thevenot et al., 2007). Aiming for an enhanced brain-bioavailability, cellular-uptake was elicited via preparation of different lipomers with varying polymer ratios, as recommended by previous studies (Yan et al., 2017). Formulations were prepared as per the components ratio sets in Table 1; with varying "drug:polymer", "Lipid:PEG", and "polymer/-drug solution:lipid/PEG solution" ratios, in search of an optimized formulation for further *in-vivo* pharmacodynamic and kinetic studies.

Lipomers, although representing a promising targeted drug carrier, their rapid clearance from bloodstream limits their application. Thereby; formulation components were neatly chosen to suit the selected preparation method and overcome any formulation design disadvantages. As adopted by the present work and recommended by previous studies, polyethylene glycol (PEG) was used as stealth camouflaging shield, to render lipomers invisible

Table 1
Lipomers composition weight ratio scheme.

Symbol	F1	F2	F3	F4	F5	F6	F7	F8	F9	F10		
Drug: Polymer	1: 1	1: 3	1: 5	3: 1	5: 1	1: 1	1: 3	1: 5	3: 1	5: 1		
Lipid: PEG			1: 1					3: 2				
Symbol	F11	F12	F13	F14	F15	F16	F17	F18	F19	F20		
Drug: Polymer	1: 1	1: 3	1: 5	3: 1	5: 1	1: 1	1: 3	1: 5	3: 1	5: 1	**1: 9 (10%w/w lipid)**	
Lipid: PEG			7: 3					4: 1				
Symbol	F21	F22	F23	F24	F25							
Drug: Polymer	1: 1	1: 3	1: 5	3: 1	5: 1							
Lipid: PEG			9: 1									
Symbol	F26	F27	F28	F29	F30	F31	F32	F33	F34	F35		
Drug: Polymer	1: 1	1: 3	1: 5	3: 1	5: 1	1: 1	1: 3	1: 5	3: 1	5: 1		**(Lipid/PEG): Polymer weight ratio**
Lipid: PEG			1: 1					3: 2				
Symbol	F36	F37	F38	F39	F40	F41	F42	F43	F44	F45		
Drug: Polymer	1: 1	1: 3	1: 5	3: 1	5: 1	1: 1	1: 3	1: 5	3: 1	5: 1	**1: 4 (20%w/w Lipid)**	
Lipid: PEG			7: 3					4: 1				
Symbol	F46	F47	F48	F49	F50							
Drug: Polymer	1: 1	1: 3	1: 5	3: 1	5: 1							
Lipid: PEG			9: 1									
Symbol	F51	F52	F53	F54	F55	F56	F57	F58	F59	F60		
Drug: Polymer	1: 1	1: 3	1: 5	3: 1	5: 1	1: 1	1: 3	1: 5	3: 1	5: 1		
Lipid: PEG			1: 1					3: 2				
Symbol	F61	F62	F63	F64	F65	F66	F67	F68	F69	F70		
Drug: Polymer	1: 1	1: 3	1: 5	3: 1	5: 1	1: 1	1: 3	1: 5	3: 1	5: 1	**3: 7 (30%w/w Lipid)**	
Lipid: PEG			7: 3					4: 1				
Symbol	F71	F72	F73	F74	F75							
Drug: Polymer	1: 1	1: 3	1: 5	3: 1	5: 1							
Lipid: PEG			9: 1									

to the immune system, hence; secure their *in-vivo* circulation half-life ($t_{1/2}$) (Khalil et al., 2013); through prohibiting phagocytic blood clearance and monophage system uptake, in addition to preventing opsonization (interaction with blood proteins), and liver sequestration, while improving system stability though optimizing surface charge (Sheng et al., 2016).

Various invasive and/or non-invasive methods have been suggested to overcome the defensive insurmountable BBB (Ahmed et al., 2014); amongst which surfactant coating have proven promising. Non-ionic surfactants, namely Tween®80, emerged as an efficient brain targeting tool, though middling in interaction between NPs and brain micro-vessel endothelial cells (Sun et al., 2004); enabling efficient targeted therapeutic delivery to brain at the right place and concentration along the desired time frame, while simultaneously reducing its accumulation at non-target sites (Etheridge et al., 2013), though reducing reticulo-endothelial system (RES) uptake, and delaying opsonization (Bender et al., 2012). In the present study 1%w/v Tween®80 was used, as recom-

mended in previous studies, for maximizing translocation of blood to brain, on minimizing accumulation of drug in liver and spleen (Wilson et al., 2008).

4.2. Characterization of nanoparticles

4.2.1. Nanoparticle morphology characterization

Importance of TEM lies in featuring lipomers' internal core-shell structure, depending on the negative stain ability to enhance electron density of lipid and lipid-PEG conjugates. Moreover; it provides preliminary indication of PS; since dynamic light scattering (DLS) technique, although fast and does not involve prior sample treatment, however, it is prone to error if particles turned to be non-uniformly spherical or have broad PDI (Valencia et al., 2010).

Micrographs of stealth lipid-polymer hybrid NPs; prepared using variable "(lecithin/PEG): PLCL" weight ratios though single-step nanoprecipitation method, are illustrated in Fig. 1; revealing their morphological characteristics. They generally appear spherical in shape with a relatively smooth surface. In addition; PLCL precipitates form the hydrophobic core, inside which the drug resides, and around which lecithin/PEG self-assemble forming PEG-coated lipid monolayer. Along the field, some indefinite aggregates are scattered. These might be resulting from the pre-examination drying process of lipomers and their associated high surface energy (Ahmad, 2017).

Furthermore; TEM revealed the mean size of particles lies within the range of 50–150 nm, together with a narrow range of variability, expressed through a PDI $\leq$ 0.2. On one side; the (1:9) and (1:4) lipomers appeared spherical and double layered of estimated particle size less than 110 nm, with the internal drug-containing polymeric core and external pegylated lipid core; indicated as dark outlining layer, as a result of negative staining of lecithin and PEG-conjugated lipids, that, in turn, enhances electron density, yielding a dim ring around the PLCL core (Chacko et al., 2018) of varying size; attributed to the amount of polymer and drug incorporated. On the other side; the (3:7) lipomers appeared as malformed aggregated particles with non-uniform surface and undifferentiated core; reflecting inappropriate composition ratios. Thereby; our study would proceed with the exclusion of the latter ratio of composition.

4.2.2. Particle size (PS) and zeta potential (ZP) studies

Particle size is a determinant factor of lipomers performance within human body, as it provides insights on circulation time and efficient passive accumulation in target sites (Perrault et al., 2009). On reviewing PS, PDI and ZP values of LTG-loaded, (Tables 2 and 3), and TX-loaded lipomers, (Tables 4 and 5), it can be observed that PS and ZP increased significantly ($p < 0.05$), on increasing polymeric or lipid content in lipomers of "(lipid/PEG): Polymer" weight ratio of (1:9) and (1:4), with mean size ranging between 31.52 ± 2.84 and 123.70 ± 4.18 nm for LTG-lipomers and 49.21 ± 4.16 and 124.60 ± 2.76 nm for TX-loaded ones; which agree with similarly reported observations in previous studies (Alexis et al., 2008). In addition, a narrow range PDI was generally observed between 0.1 and 0.2, inferring the system's excellent homogeneity. As discussed earlier; the presented PS and PDI results lie within the identified optimum standards; favorable for systemic drug delivery and beneficial in effectively prolonging lipomers circulation time, BBB targeting and residence (Zhao et al., 2015).

The presented analysis showed that increasing the total polymeric content within lipomeric structure, resulted in an increase in NPs size as shown in tables (2–5). This increase in particle size is attributed to the high molecular weight of various polymers included within NPs structure (PEG and PLCL), and the resulting increase in dispersed phase viscosity (Ahmad et al., 2018a).

Tuning surface ZP is crucial for lipomers *in-vitro* and *in-vivo* stability optimization; where high ZP values would yield highly electrostatically stable lipomers *in-vitro*, as a result of electro-kinetic potential between NPs surface and bulk solution, however; this does not guarantee a consequent *in-vivo* immuno-compatibility. An optimal surface charge should, thereby, provide balance between lipomers *in-vitro* stability and *in-vivo* immuno-compatibility (Salvador-Morales et al., 2009).

Owing to the negatively charged lecithin, ester terminated PLCL; represented through the uncapped carboxylic group (Song et al., 2011), and the non-ionic/slightly negative PEG (Sheng et al., 2016); lipomers generally possessed high negative ZP values ranging between (−30.11 ± 1.23 and −73.13 ± 1.46 mV) for LTG-lipomers, and (−35.63 ± 3.55 and −80.30 ± 2.99 mV), for TX lipomers indicating high system stability. Furthermore; no significant difference, ($p \geq 0.05$), in either PS or ZP was noticed on increasing the initially loaded drug amount of the same formulations. This can be attributed to compact structures in which polymers precipitate during the process of nanoprecipitation; forming a relatively inflexible core with identified inner volume, in which specified amount of drug can be entrapped (Zhang et al., 2007).

Briefly, it can be concluded that a stable lipomer system was achieved with "(lipid/PEG):Polymer" weight ratio of (1:9) and (1:4), which comes in accordance with TEM micrographs previously presented in Fig. 1, and results reported in previous studies (Badran et al., 2017), where the amount of lipid, at such ratios, is believed to sufficiently cover the entire polymeric hydrophobic core, however, further increase in lipid content would depass its critical micelle concentration (CMC), resulting in structural shift from lipomers to lecithin liposomes; whose coexistence would cause an overall increase in size and decrease in ZP. Thereby; on lowering such weight ratio to specified limits: below the CMC of lecithin, liposomes would not be formed, as per dynamic light scattering measurements, resulting in a consequent decrease in PS and increase ZP (Gu et al., 2008).

4.2.3. Drug loading (DL) and entrapment efficiency (EE)

Pegylated lipomers are generally known for high DL capacities, due to their PEG surface coating which prevents drug leakage along the preparation process (Sheng et al., 2016). Moreover; electrostatic interaction between drugs (LTG and TX) and lipomer surface is suggested, leading to adsorption (Song et al., 2011), reflected through high DL capacity. This was practically pronounced though results presented in tables (2–5); where DL mean values of LTG-lipomers (Tables 2 and 3), ranged between 28.85 ± 2.91 and 84.73 ± 2.03%, as for TX-lipomers (Tables 4 and 5); DL lied between 29.82 ± 2.49 and 91.45 ± 1.36%. It is worth noting that lipophilicity of both LTG and TX resulted in a significant increase in DL, ($p < 0.05$), on increasing drug and/or lipid content, however, increasing its polymeric content had no effect, ($p \geq 0.05$). Similar conclusion was previously reported (Ahmad et al., 2019). This can be justified though the possible formation of a less hydrophobic core of PLCL-PEG di-block copolymer, on increasing PLCL content, as a result of a believed interaction between some PEG blocks and excess PLCL during nanoprecipitation process (De Miguel et al., 2000).

Lipomers EE generally increased, ($p < 0.05$), as a function of increasing polymer, lipid, and/or drug content incorporated; where lipomers with "lecithin:PEG" ratio of (9:1), and "lipid/PEG:PLCL" ratio of (1:4), possessed the maximum EE; where no further significant increase, ($p \geq 0.05$), in EE was noticed on increasing drug or polymer content. Mean EE values of LTG-lipomers, in Tables 2 and 3, ranged between 45.23 ± 2.21 and 99.61 ± 1.45%, as for TX-lipomers, their EE mean values, shown in Tables 4 and 5, ranged between 53.11 ± 2.16 and 99.75 ± 1.20%. Results generally agreed with data reported in literature about the molecular fence drug
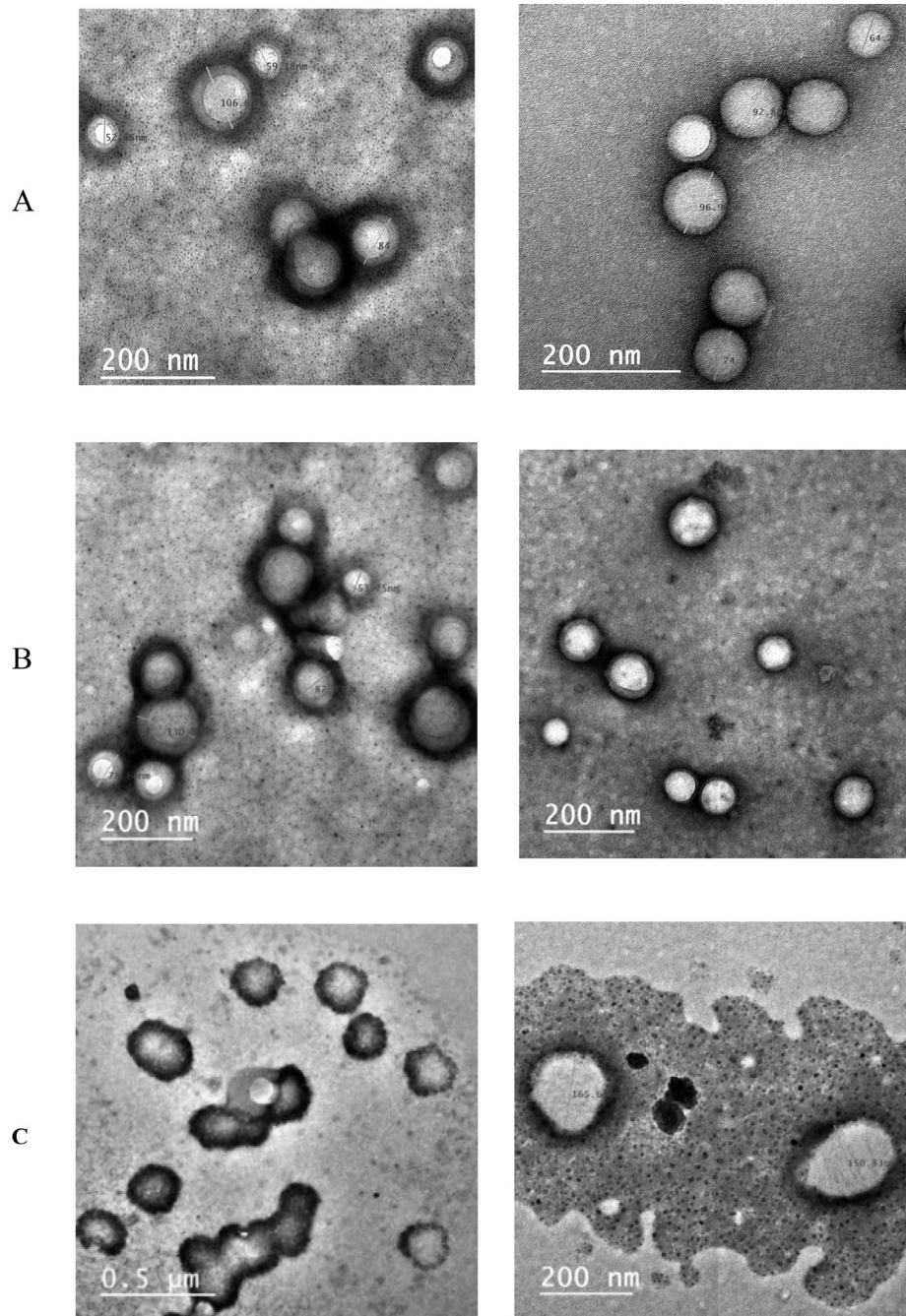
Fig. 1. Transmission electron micrographs of stealth lipomers of various (lipid/PEG): Polymer weight ratios: (a) 1:9, (b) 1:4, (c) 3:7.

retention mechanism of lipid monolayer at the PLCL core/ PEG shell interface; which is thought to improve both EE and DL though preventing free diffusion of small drug molecules out of the polymeric core, and reducing water penetration rate into it, leading to consequent decrease in polymer hydrolysis rate, thus; slowing down drug release from NPs (Wong et al., 2006).

4.3. In-vitro release study and kinetics

On reviewing system characterization results presented in tables (2–5), it can be concluded that lipomers of both drugs possessed optimum PS and PDI values, and proved stable though high ZP values. Thereby; based on DL and EE values, lipomers with "drug:PLCL" ratio of (5:1), and interchangeable "lecithin: PEG" and ["lipid/PEG":PLCL] ratios were selected for further *in-vitro*

release studies; as they showed the highest DL and EE values. Such formulations are: LF5, LF10, LF15, LF20, LF25, LF30, LF35, LF40, LF45, and LF50, and their TX-loaded homologues.

Results demonstrated in Fig. 2 show that LTG was released from all lipomers according to Korsmeyer-Peppas kinetic model, with the exception of LF15, LF20 and LF40, where Baker-Lonsdale model was prevailing. It can be observed from Fig. 3 that TX release from homologous lipomers followed the same kinetic models. Thereby, it can be concluded that formulation structure and inter-component ratio has the upper hand in specifying release kinetics of both drugs regardless to differences in their chemical structure and degree of lipophilicity.

Among LTG-loaded lipomers, LF20 showed significantly, ($p < 0.05$) the highest release efficiency ($81.49 \pm 3.22\%$), followed by the non-significantly different, ($p \geq 0.05$), LF15

Table 2
Particle size, polydispersity index, zeta potential, loading and entrapment efficiency of lamotrigine-loaded lipomers with (lipid/PEG): Polymer weight ratio of (1:9).

Symbol	Mean PS[a] (nm ± SD)	Mean PDI[b]	Mean ZP[c] (mV ± SD)	Mean DL[d] (% ± SD)	Mean EE[e] (% ± SD)
LF1	31.52 ± 2.84	0.10	−30.11 ± 1.23	28.85 ± 2.91	45.23 ± 2.21
LF2	44.65 ± 2.35	0.20	−37.59 ± 2.21	30.70 ± 3.12	51.77 ± 2.34
LF3	58.91 ± 3.78	0.17	−42.31 ± 2.00	31.56 ± 3.84	59.05 ± 2.43
LF4	33.70 ± 3.12	0.15	−31.00 ± 3.42	34.53 ± 1.21	55.85 ± 1.93
LF5	35.02 ± 4.29	0.11	−32.14 ± 3.98	38.82 ± 2.04	60.41 ± 2.12
LF6	38.04 ± 3.72	0.10	−35.40 ± 2.88	35.31 ± 3.41	51.75 ± 3.26
LF7	56.41 ± 2.21	0.10	−41.50 ± 1.01	37.53 ± 3.19	59.03 ± 3.21
LF8	79.27 ± 3.46	0.12	−46.86 ± 3.72	39.80 ± 3.30	67.10 ± 3.62
LF9	41.66 ± 3.86	0.10	−37.11 ± 2.86	41.38 ± 1.26	60.09 ± 1.90
LF10	43.01 ± 4.00	0.16	−39.17 ± 2.13	48.14 ± 2.06	65.05 ± 2.18
LF11	47.35 ± 5.83	0.12	−39.04 ± 2.54	40.17 ± 2.11	59.73 ± 3.15
LF12	67.92 ± 3.81	0.10	−44.91 ± 3.81	40.60 ± 2.83	68.01 ± 3.80
LF13	84.01 ± 4.73	0.11	−49.77 ± 2.00	41.61 ± 1.32	74.39 ± 2.42
LF14	52.75 ± 6.02	0.15	−40.15 ± 2.97	45.13 ± 3.42	71.61 ± 2.91
LF15	57.62 ± 2.40	0.14	−42.92 ± 3.49	51.25 ± 2.33	80.63 ± 4.07
LF16	60.44 ± 4.25	0.13	−47.55 ± 3.13	45.51 ± 2.14	68.23 ± 3.12
LF17	78.58 ± 4.52	0.12	−52.76 ± 1.25	46.04 ± 2.30	77.86 ± 2.53
LF18	98.32 ± 4.90	0.10	−56.13 ± 5.18	46.97 ± 2.11	85.26 ± 3.72
LF19	67.93 ± 5.71	0.16	−47.69 ± 3.10	49.83 ± 1.58	79.42 ± 3.86
LF20	75.82 ± 6.42	0.14	−49.00 ± 2.54	57.53 ± 2.07	87.78 ± 1.49
LF21	87.20 ± 5.02	0.13	−55.80 ± 2.33	49.65 ± 2.38	80.60 ± 2.85
LF22	99.40 ± 4.06	0.11	−62.55 ± 1.18	50.56 ± 3.25	87.32 ± 3.19
LF23	117.86 ± 3.98	0.10	−66.02 ± 2.29	51.26 ± 1.76	94.00 ± 2.20
LF24	91.63 ± 4.06	0.15	−56.19 ± 1.47	58.46 ± 1.32	94.03 ± 1.67
LF25	98.72 ± 6.78	0.15	−57.13 ± 2.93	66.51 ± 2.13	98.52 ± 1.19

[a] PS (particle size).
[b] PDI (polydispersity index).
[c] ZP (zeta potential).
[d] DL (drug loading).
[e] EE (entrapment efficiency).

Table 3
Particle size, polydispersity index, zeta potential, loading and entrapment efficiency of lamotrigine-loaded lipomers with (lipid/PEG): Polymer weight ratio of (1:4).

Symbol	Mean PS[a] (nm ± SD)	Mean PDI[b]	Mean ZP[c] (mV ± SD)	Mean DL[d] (% ± SD)	Mean EE[e] (% ± SD)
LF26	45.77 ± 2.43	0.10	−39.40 ± 3.57	42.07 ± 2.27	53.17 ± 3.02
LF27	66.22 ± 4.71	0.11	−44.98 ± 1.51	42.98 ± 2.05	59.51 ± 2.73
LF28	80.71 ± 3.15	0.13	−48.70 ± 2.49	43.12 ± 3.22	65.24 ± 3.54
LF29	52.06 ± 3.44	0.12	−40.00 ± 2.36	48.05 ± 1.70	67.18 ± 2.36
LF30	58.31 ± 2.28	0.11	−40.50 ± 1.50	55.51 ± 1.18	76.26 ± 2.40
LF31	54.21 ± 3.62	0.13	−46.46 ± 2.95	48.36 ± 2.16	68.27 ± 1.47
LF32	75.62 ± 3.99	0.11	−51.16 ± 1.27	48.75 ± 1.70	76.92 ± 3.12
LF33	96.10 ± 5.20	0.15	−55.90 ± 2.69	48.58 ± 1.37	82.53 ± 1.98
LF34	61.88 ± 4.08	0.12	−47.00 ± 2.88	54.00 ± 2.14	79.03 ± 1.42
LF35	71.34 ± 3.38	0.14	−48.12 ± 2.51	58.72 ± 1.02	85.18 ± 2.11
LF36	70.25 ± 5.11	0.14	−52.85 ± 2.34	57.68 ± 1.95	78.53 ± 2.61
LF37	92.15 ± 6.48	0.12	−58.07 ± 2.44	58.12 ± 2.11	86.72 ± 3.54
LF38	113.67 ± 3.82	0.12	−65.30 ± 1.73	58.61 ± 2.19	93.31 ± 1.27
LF39	81.41 ± 4.36	0.16	−53.21 ± 2.65	63.09 ± 1.90	90.11 ± 2.02
LF40	93.52 ± 6.89	0.16	−54.93 ± 1.33	68.16 ± 2.31	97.43 ± 3.81
LF41	84.13 ± 4.85	0.10	−57.15 ± 4.65	61.32 ± 2.63	91.70 ± 1.22
LF42	99.92 ± 5.72	0.13	−64.33 ± 2.62	62.04 ± 2.28	95.93 ± 1.41
LF43	120.05 ± 6.18	0.10	−69.61 ± 2.78	63.53 ± 2.14	98.59 ± 1.50
LF44	93.49 ± 3.66	0.15	−59.28 ± 1.95	72.92 ± 2.83	94.82 ± 1.11
LF45	99.26 ± 4.08	0.12	−60.59 ± 2.18	79.74 ± 2.91	98.64 ± 1.45
LF46	95.14 ± 3.85	0.14	−64.77 ± 3.52	70.00 ± 2.59	97.23 ± 2.70
LF47	110.29 ± 4.39	0.17	−69.10 ± 1.12	72.14 ± 3.23	97.55 ± 3.02
LF48	123.70 ± 4.18	0.11	−73.13 ± 1.46	72.81 ± 2.92	99.62 ± 2.00
LF49	100.52 ± 5.52	0.10	−64.80 ± 1.28	78.56 ± 1.73	98.28 ± 2.31
LF50	114.76 ± 5.16	0.10	−66.69 ± 2.62	84.73 ± 2.03	99.61 ± 1.45

[a] PS (particle size).
[b] PDI (polydispersity index).
[c] ZP (zeta potential).
[d] DL (drug loading).
[e] EE (entrapment efficiency).

Table 4
Particle size, polydispersity index, zeta potential, loading and entrapment efficiency of tenoxicam-loaded lipomers with (lipid/PEG): Polymer weight ratio of (1:9).

Symbol	Mean PS[a] (nm ± SD)	Mean PDI[b]	Mean ZP[c] (mV ± SD)	Mean DL[d] (% ± SD)	Mean EE[e] (% ± SD)
TF1	49.21 ± 4.16	0.10	−35.63 ± 3.55	29.82 ± 2.49	53.11 ± 2.16
TF2	56.04 ± 4.99	0.15	−40.42 ± 2.11	30.61 ± 3.15	58.98 ± 1.45
TF3	61.42 ± 2.31	0.18	−45.11 ± 2.31	31.56 ± 2.73	63.87 ± 2.42
TF4	52.35 ± 4.29	0.11	−37.36 ± 3.95	37.73 ± 2.03	66.29 ± 1.93
TF5	53.55 ± 3.81	0.14	−39.88 ± 2.38	42.98 ± 2.58	74.82 ± 2.76
TF6	57.75 ± 4.03	0.18	−40.37 ± 1.92	43.04 ± 1.22	69.46 ± 2.11
TF7	65.24 ± 2.10	0.11	−44.12 ± 2.14	43.00 ± 2.35	76.33 ± 1.02
TF8	70.10 ± 4.74	0.10	−49.70 ± 1.33	43.83 ± 1.33	81.72 ± 2.98
TF9	60.50 ± 3.88	0.19	−41.39 ± 2.51	49.09 ± 2.27	77.22 ± 1.41
TF10	62.82 ± 4.05	0.14	−42.69 ± 3.46	54.13 ± 1.45	82.48 ± 1.54
TF11	79.41 ± 3.18	0.14	−43.78 ± 2.72	57.82 ± 2.48	75.46 ± 2.43
TF12	87.56 ± 1.98	0.12	−47.45 ± 1.84	58.11 ± 1.19	79.27 ± 1.12
TF13	95.34 ± 2.37	0.16	−50.65 ± 1.57	58.54 ± 1.93	83.15 ± 2.07
TF14	80.54 ± 3.12	0.13	−43.10 ± 2.11	65.90 ± 2.48	84.76 ± 1.87
TF15	82.26 ± 2.42	0.10	−43.43 ± 2.77	70.10 ± 2.99	88.91 ± 1.00
TF16	88.52 ± 4.61	0.15	−48.35 ± 3.36	69.15 ± 2.54	83.66 ± 2.72
TF17	95.87 ± 2.75	0.14	−54.06 ± 1.64	70.84 ± 1.19	87.28 ± 1.31
TF18	103.67 ± 3.72	0.16	−57.20 ± 1.82	70.42 ± 2.74	91.53 ± 1.08
TF19	90.30 ± 4.21	0.17	−49.94 ± 3.10	76.66 ± 3.16	87.13 ± 1.32
TF20	93.20 ± 4.94	0.12	−49.72 ± 2.16	81.91 ± 2.46	93.82 ± 1.18
TF21	106.45 ± 3.16	0.15	−53.58 ± 2.50	80.03 ± 2.62	89.12 ± 2.62
TF22	114.85 ± 1.63	0.17	−57.43 ± 2.92	82.34 ± 1.55	93.25 ± 1.68
TF23	121.23 ± 1.62	0.14	−61.09 ± 1.58	82.12 ± 1.87	98.91 ± 2.03
TF24	107.58 ± 2.70	0.15	−54.29 ± 2.90	89.02 ± 2.13	94.82 ± 1.40
TF25	109.48 ± 4.01	0.10	−55.23 ± 3.14	95.53 ± 3.29	99.27 ± 1.13

[a] PS (particle size).
[b] PDI (polydispersity index).
[c] ZP (zeta potential).
[d] DL (drug loading).
[e] EE (entrapment efficiency).

Table 5
Particle size, polydispersity index, zeta potential, loading and entrapment efficiency of tenoxicam-loaded lipomers with (lipid/PEG): Polymer weight ratio of (1:4).

Symbol	Mean PS[a] (nm ± SD)	Mean PDI[b]	Mean ZP[c] (mV ± SD)	Mean DL[d] (% ± SD)	Mean EE[e] (% ± SD)
TF26	80.20 ± 1.06	0.13	−48.90 ± 2.50	34.65 ± 2.93	65.24 ± 2.15
TF27	86.23 ± 2.59	0.12	−53.30 ± 1.77	36.11 ± 3.14	70.19 ± 1.42
TF28	92.29 ± 3.72	0.17	−56.50 ± 1.04	38.45 ± 3.52	75.81 ± 2.43
TF29	81.15 ± 2.11	0.10	−49.22 ± 1.56	42.27 ± 2.95	72.52 ± 3.07
TF30	83.13 ± 3.75	0.13	−49.19 ± 1.53	48.22 ± 2.49	77.21 ± 2.22
TF31	85.10 ± 3.50	0.11	−55.25 ± 2.61	41.20 ± 2.57	72.38 ± 2.64
TF32	91.97 ± 2.94	0.15	−59.82 ± 3.20	41.63 ± 3.71	78.89 ± 1.45
TF33	96.38 ± 1.92	0.12	−63.33 ± 2.19	43.94 ± 2.27	83.99 ± 2.44
TF34	88.14 ± 4.74	0.15	−56.52 ± 3.60	54.17 ± 3.19	81.45 ± 2.35
TF35	89.37 ± 2.33	0.16	−57.31 ± 2.44	60.39 ± 2.64	86.12 ± 2.04
TF36	90.23 ± 3.20	0.12	−61.85 ± 1.90	48.16 ± 3.51	80.90 ± 3.16
TF37	96.28 ± 1.26	0.11	−66.37 ± 1.52	48.14 ± 2.79	86.51 ± 2.50
TF38	103.79 ± 2.43	0.10	−69.21 ± 1.13	52.56 ± 2.08	91.23 ± 2.33
TF39	91.11 ± 2.62	0.13	−63.14 ± 2.24	57.72 ± 3.66	88.63 ± 2.08
TF40	93.31 ± 4.27	0.13	−63.81 ± 2.23	66.19 ± 2.10	93.72 ± 1.59
TF41	96.82 ± 2.45	0.14	−68.20 ± 2.11	54.78 ± 2.40	90.16 ± 2.76
TF42	102.64 ± 1.81	0.18	−72.25 ± 3.06	55.76 ± 3.72	94.13 ± 1.48
TF43	115.54 ± 2.55	0.11	−77.04 ± 3.91	56.94 ± 2.43	97.04 ± 1.82
TF44	98.10 ± 3.53	0.15	−69.73 ± 2.14	64.56 ± 1.85	95.70 ± 1.21
TF45	98.55 ± 3.88	0.13	−69.23 ± 2.00	72.52 ± 3.11	98.98 ± 2.03
TF46	109.31 ± 2.33	0.19	−74.21 ± 1.90	69.74 ± 3.38	97.59 ± 1.78
TF47	119.41 ± 3.68	0.11	−78.36 ± 2.15	71.19 ± 2.76	98.13 ± 2.40
TF48	124.60 ± 2.76	0.10	−80.30 ± 2.99	72.43 ± 2.94	98.80 ± 1.80
TF49	109.45 ± 3.12	0.13	−75.03 ± 2.06	84.79 ± 2.70	99.23 ± 1.06
TF50	111.27 ± 3.42	0.16	−76.05 ± 2.41	91.45 ± 1.36	99.75 ± 1.20

[a] PS (particle size).
[b] PDI (polydispersity index).
[c] ZP (zeta potential).
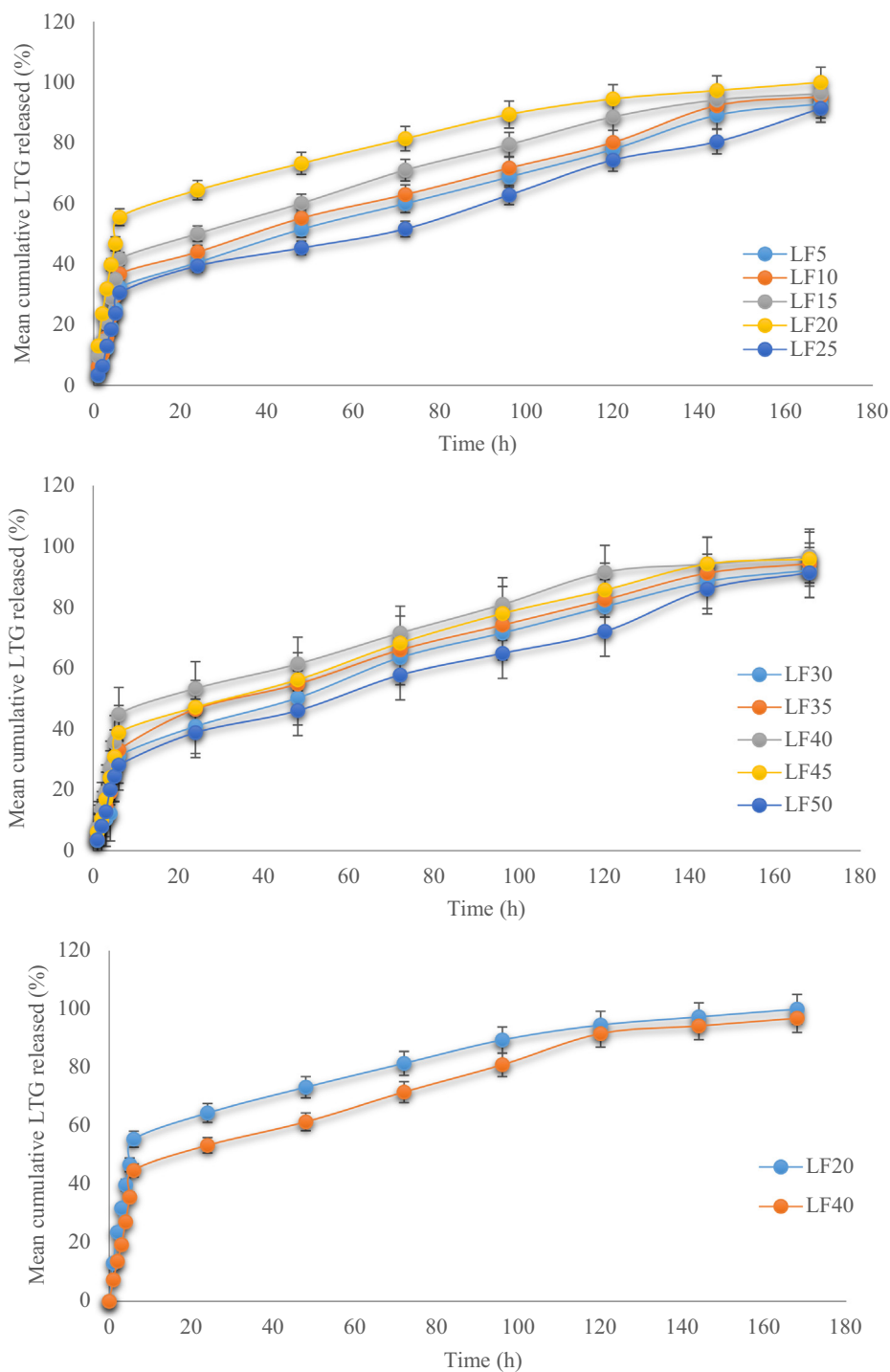[d] DL (drug loading).
[e] EE (entrapment efficiency).

Fig. 2. *In-vitro* release profiles of selected LTG loaded lipomers in phosphate buffer solution (pH 7.4).

(72.29 ± 2.48%), LF40 (73.81 ± 3.09%), and LF45 (70.07 ± 1.35%), then the non-significantly different lipomers RE values ranging between 58.47 ± 5.70% (LF25) and 67.53 ± 2.13% (LF35). Similarly, for TX-loaded lipomers, TF20 possessed significantly, (p < 0.05), the highest RE (77.61 ± 2.25%), followed by non-significantly different, (p ≥ 0.05), RE values ranging between 68.71 ± 3.72% (TF15) and 51.70 ± 3.94% (TF5).

On reviewing MDT values of LTG and TX loaded lipomers, the inversely proportional relationship between MDT and RE was obvious where LF20 and TF20 showed the minimum MDT values, each compared to its drug lipomers; 31.00 ± 2.58 and 37.12 ± 1.64 h,

respectively. These results come in accordance with physical properties reported by FDA for LTG and TX molecules, as BCS class II drugs; where the former is relatively less lipophilic, as per its two ring relatively lower molecular weight structure compared to the latter's thee ringed higher molecular weight structure, reflected though lower logP and higher pKa values 1.87 and 5.7, respectively, of LTG compared to 2.42 and 4.26, respectively, for TX.

There are general factors that would affect drug release profile from lipomers, including drug/polymer interaction, drug solubility, polymer degradation rate, and PS. If the drug was physically
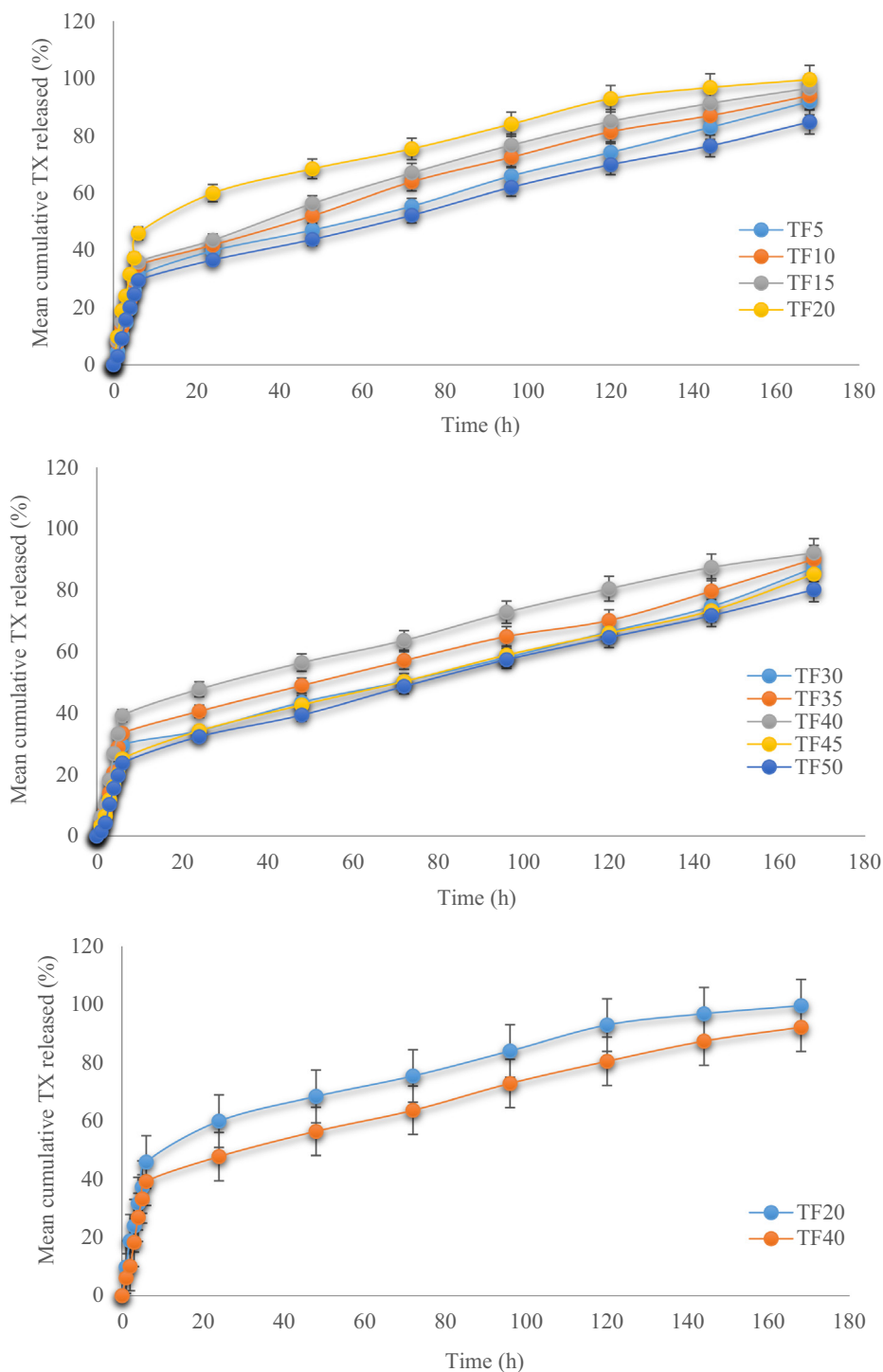
Fig. 3. *In-vitro* release profiles of selected TX loaded lipomers in phosphate buffer solution (pH 7.4).

encapsulated within the polymeric core, they would be consequently released though diffusion and polymer erosion; while release of chemically conjugated drugs would be a function of drug-polymer chains hydrolysis and subsequent drug diffusion (Aryal et al., 2010).

The F20 lipomer composed of ["lecithin/PEG":PLCL] ratio of 1:9, (drug:polymer) ratio of 5:1, and (lecithin:PEG) ratio of 4:1, was selected for its superior properties for loading L-Dopa in a comparative lipomer structure, as shown in Fig. 4. On comparing the three drug-loaded L20 lipomers, it is clear that L-Dopa was similarly

released according to Baker-Lonsdale kinetic model, which assures the dominant effect of lipomer composition over the drug release behavior. Inspite of its hydrophilicity and comparatively low molecular weight, L-Dopa showed significantly, ($p < 0.05$), the minimum comparative RE ($70.96 \pm 2.03\%$), and consequent maximum, ($p < 0.05$), MDT value (41.09 ± 1.30 h). This can be attributed to its high pKa value (9.06); making the release media relatively unfavorable.

On comparing release of L-Dopa from Sinemet® and LDF20, a Weibull kinetic model was observed by the former, with signifi-
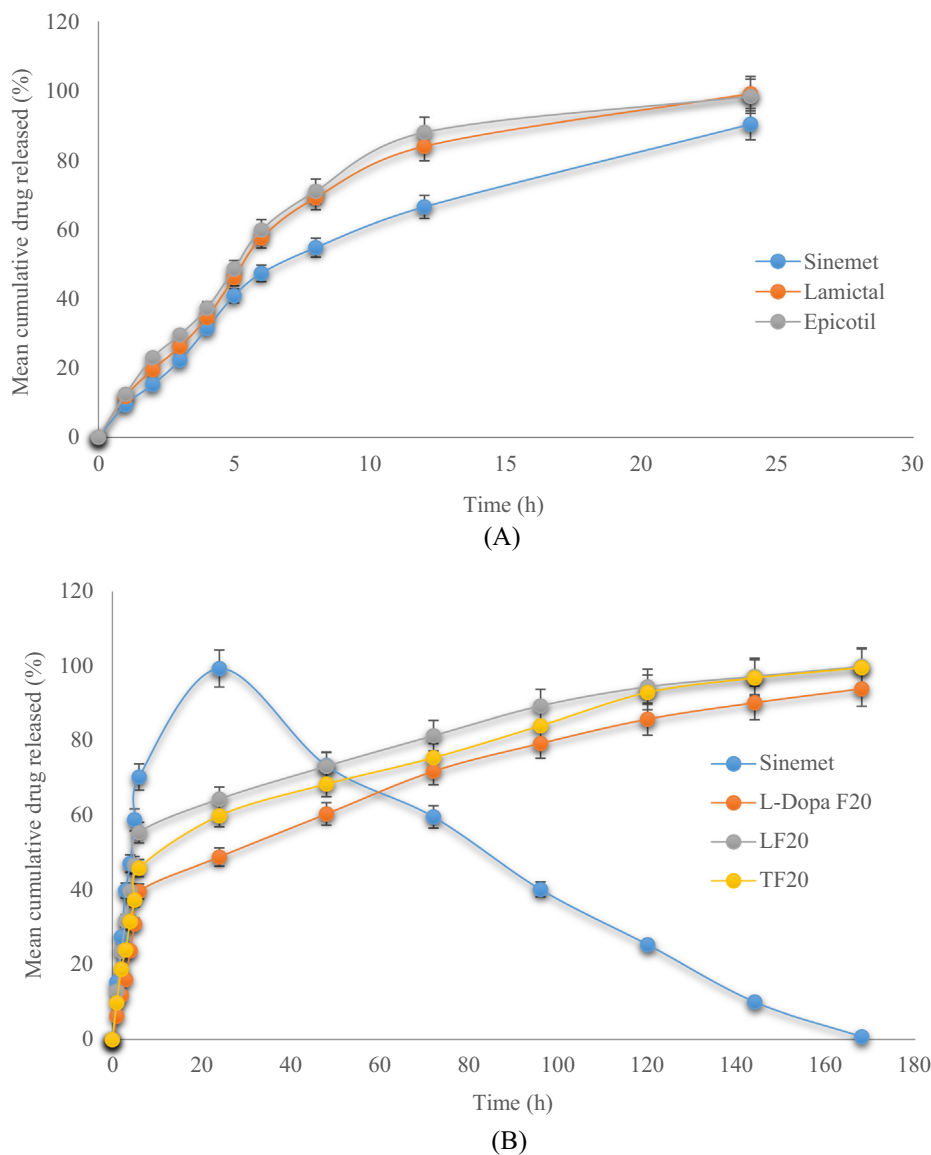
Fig. 4. (A) Comparative *in-vitro* release of lamotrigine, tenoxicam and L-Dopa from corresponding marketed tablets: Lamictal, Epicotil and Sinemet, respectively in gastrointestinal tract gradient pH values, (B) *in-vitro* release of L-Dopa from Sinemet tablet and DF20 compared to LF20 and TF20 in phosphate buffer solution (pH 7.4).

cantly, (p < 0.05), lower RE of 59.51 ± 3.71%, and a significantly higher MDT (p < 0.05), reaching the double; 81.93 ± 5.17 h. Release of LTG and TX from their respective marketed tablets showed non-significant, (p ≥ 0.05), RE of both: 70.77 ± 4.55 and 72.84 ± 3.62%, respectively. Generally, comparing marketed formulations to their lipomer homologues infer the efficiency of the designed lipomer in providing a slow release profile of the thee drugs *in-vitro*, from which a likewise attitude is expected *in-vivo*.

4.4. In-vitro stability

High (surface area:volume) ratio associated with NPs makes them prone to *in-vivo* aggregation, since high NPs concentration significantly excel particle–particle interaction governed by Van der Waals forces. Thus; selected lipomers were investigated for stability in different sera, as an indicator for their *in-vivo* efficiency as drug carriers. Hence; the scope of this test differs totally from the common shelf-life stability test; where detection of PS, and PDI changes would be a surrogate for protein adsorption and bio-fouling (Sheng et al., 2016). Furthermore; ZP is a critical *in-vitro*

stability indicator that would give insights about the optimum "lipid:PEG" ratio (Alexis et al., 2008). It is worth mentioning that diluted serum and not a whole one is used, to avoid any possible interference with PS and PDI measuring, due to high protein and protein aggregate content in whole serum; where unstable formulations would tend to quickly adsorb serum proteins, forming aggregates, resulting in misleading large PS and broad PDI range (Cheng et al., 2010).

From Figs. 5 and 6, all tested lipomers and PLCL/PEG controls proved stable in both 10 wt% BSA and human plasma solutions; with no significant differences reported, (p ≥ 0.05), in their initially measured PS, PDI or ZP values along the experiment time intervals. As for PLCL controls, a highly significant increase, (p < 0.05), in the thee investigated values were reported within 30 min of their incubation in both test media; which could be justified as per the role of PEG in maintaining lipomer stability, both *in-vitro*; by reducing aggregation, and *in-vivo*; by evading RES and immune system recognition, in addition to preventing protein adsorption, and bio-fouling (Moghimi and Szebeni, 2003). Particles with ZP ≤ 30 mV or ≥ 30 mV are usually perceived as stable for *in-vitro* shelf-life

storage though electrostatic repulsive forces, however; additional steric repulsive forces are required to act synergistically with the former stabilizing forces, to assure provide system biological stability. For lipomers; PEG molecules are the key donators of steric repulsion; where Chan et al. found that the highest stability of was achieved at 15 wt% "lipid:polymer" mass ratio and 7.5:2.5 "lipid:PEG" molar ratio (Chan et al., 2009).

Briefly; all investigated lipomers proved stable, however; only those having best release kinetic profiles, one in a group, were selected for further characterization: LF20, LF40, TF20, TF40, LDF20, and LDF40.

4.5. In-vitro biocompatibility "Cytotoxicity"

Cytotoxicity is generally studied to examine the carrier and drug *in-vivo* biocompatibility to cell vitality. Unlike other NP systems; lipomers have been documented as efficient drug reserve carriers, due to their controlled gradual drug unleashing
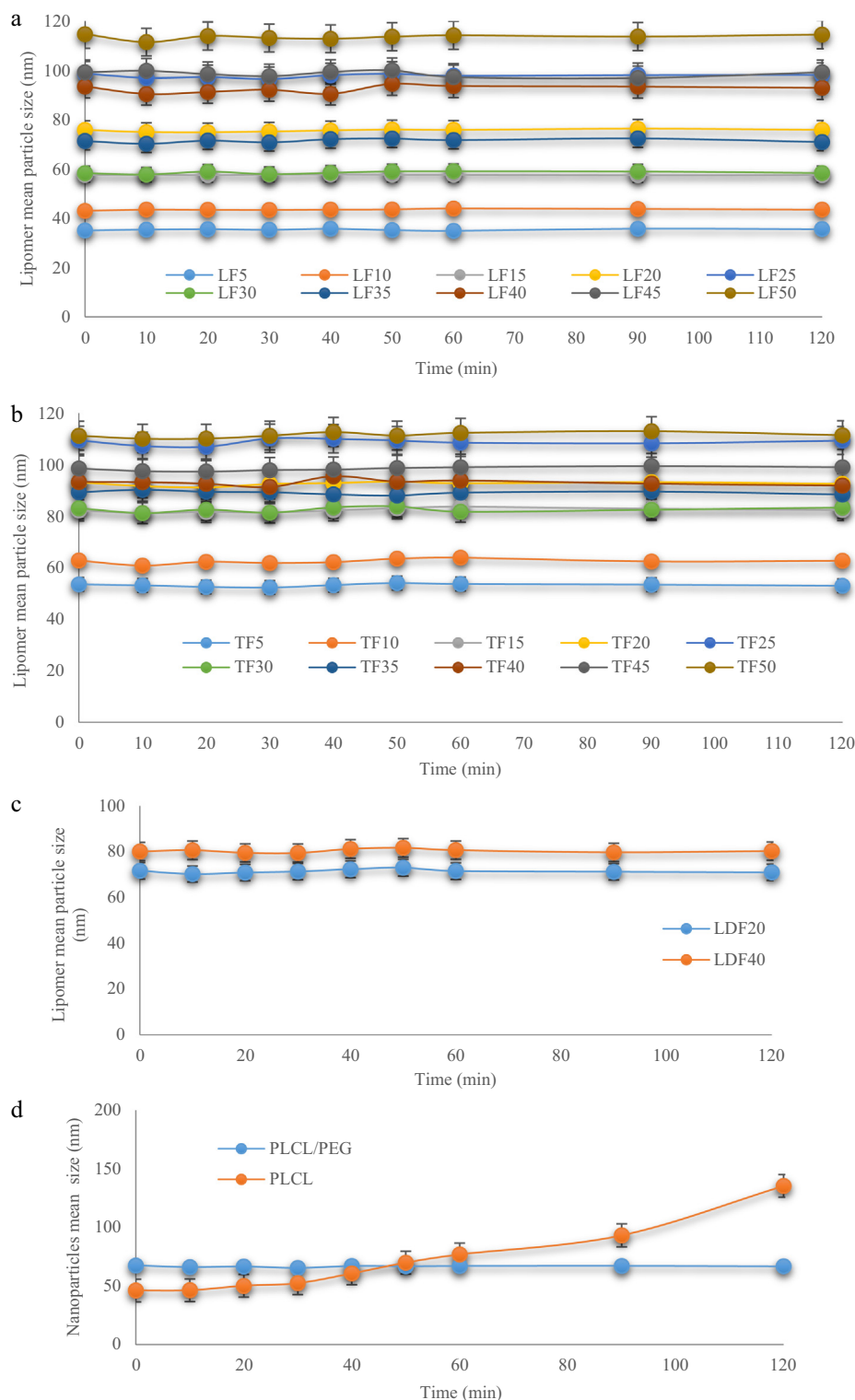
Fig. 5. Lipomers size temporal stability *in-vitro* with 10 wt% Bovine Serum Albumin at 37 °C (a) lamotrigine, (b) tenoxicam, (c) L-Dopa, (d) control.
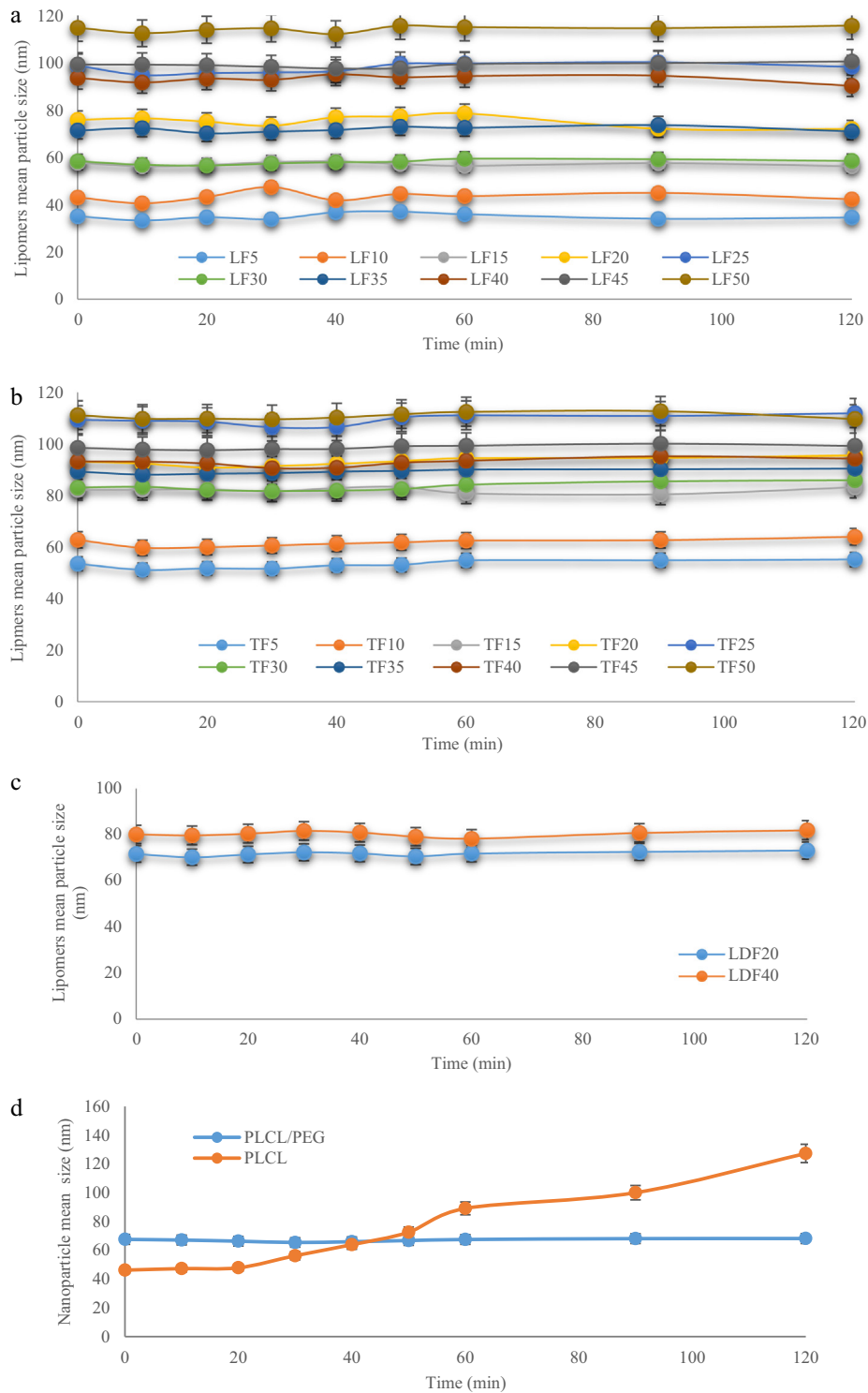
Fig. 6. Lipomers size temporal stability *in-vitro* 10 wt% plasma with heparin at 37 °C (a) lamotrigine, (b) tenoxicam, (c) L-Dopa, (d) control.

properties, whereas; other NPs, are accused of probable cytotoxicity, since drug might be subject to bolus release once internalized by diseased cells. However; although, non-ionic surfactants are generally reported as less toxic compared to ionic ones, a number of adverse effects has been previously reported for NP formulations attributed to their surfactant content. Thereby; in the present study, cytoxicity of drugs, PEG and Tween®80 of the selected lipomers was assessment, to avoid any probable *in-vivo* toxicity related

effects associated to the present pharmaceutical design (Gursoy et al., 2003).

To assess cell viability, different concentrations of Tween®80 were examined (1, 3, 5, and 10 %w/v) for coating LF20, TF20 and LDF20, with drug concentration adjusted at doses equivalent to their respective marketed tablets, versus unloaded F20 (control) for each Tween®80 concentration. The CellTiter 96® AQ$_{ueous}$ Non-Radioactive Cell Proliferation Assay is a colorimetric method for

determining the number of viable cells in response to foreign carriers/drugs, thus; assuring the latter's biocompatibility, depending on water soluble tetrazolium inner salt referred to as MTS, and an electron coupling reagent (phenazine methosulphate; PMS); both forming the "MTS reagent" which is bio-reduced in viable metabolically active cells, via its dehydrogenase enzymes, into aqueous Formazan product soluble in the culture medium (Barltrop et al., 1991). Quantity of Formazan product, inferred though its absorbance at 490 nm, can be directly measured from assay plates; where absorbance is directly proportional to number of viable cells in culture, without any need for further processing, compared to the previously used MTT assay (Bahuguna et al., 2017).

Results presented in Fig. 7 show that none of the tested lipomers were cytotoxic neither at the employed PEG concentration nor at 1 and 3%w/v Tween®80 concentrations, however; toxicity was noticed at 5 and 10%w/v of the latter. Such findings agree with data reported in literature about Tween®80 cytotoxicity; where 5% w/v Tween®80 exhibited certain cytotoxicity that increased proportionally with its concentration. Furthermore; the 100% viability of the F20 control proves the biocompatibility of lecithin (Lv et al., 2006), PEG and PLCL at the given concentration ratios. In addition; the 100% biocompatibility of the uncoated drug loaded lipomers proves safety of the administered dose of each drug, as reported in literature (Gonzalez-Carter et al., 2019).

From the presented cytotoxicity experiment, it can be concluded that no significant difference, ($p \geq 0.05$), in cytotoxicity in any of LF20, TF20 and LDF20 was observed compared to drug-free or drug-loaded controls. In addition, cytotoxicity was more pronounced in BBB cells compared to human brain cells, when treated similarly; where no significant differences, ($p \geq 0.05$) were observed in cytotoxicity up to 3%w/v in either cell-lines, while significance, ($p < 0.05$), was obvious at Tween®80 concentrations $\geq 5\%$ w/v. It is also worth noting that any SD reported might be attributed to slight spontaneous absorbance in the culture medium incubated with MTS reagent; where type of culture medium and serum, pH and length of light exposure are variables that may contribute to background absorbance; typically 0.2–0.3 absorbance units after 4 h (CellTiter 96, xxxx).

4.6. In-vivo pharmacokinetic studies

Although lipomers structural flexibility provide a wide array for optimizing desirable *in-vivo* pharmacokinetics, only limited *in-vivo* pharmacokinetic and dynamic data is available in literature, inspite of extensive cell culture experiments reported (Zhang and Zhang, 2010). In this study, a full *in-vivo* profile is presented; providing insights about lipomers targeting efficiency and subsequent therapeutic efficacy as drug carriers (Hong et al., 2009).

For HPLC-UV analysis, each of LTG, TX and L-Dopa and their respective IS solutions spiked at high intensity, with no interfering endogenous peaks or noise observed, indicating method specificity. Retention time recorded for each in rat plasma and brain homogenate, came in accordance with similar data reported in literature (Martins et al., 2013). All standard calibration curves assessed in rat plasma and brain homogenate indicated linear relation between drug-plasma and/or drug-brain concentration and the input concentration, with coefficient of determination (R^2) approaching unity; inferring linearity. Assessing drug extraction recovery from rat plasma and brain homogenate, proved assay sensitivity, reproducibility, precision, consistency, specificity and accuracy as per data presented in the "supporting documents".

After administration of various formulations as designed, release of drugs was tracked along a week time scale in rat plasma and brain homogenate, compared to placebo controls. Fig. 8A1 indicates that, almost; none of the drugs appeared in plasma after IV administration; which compiles with the desired properties of

designed lipomers; intended for sustained release of drugs in their target site. Fig. 8A2; presents a zoomed-in portion of the main figure, with trivial concentrations of each drug noticed; probably attributed to free drug surface adsorption. As for standard tablets, shown in Fig. 8B, LTG, TX, and LD were observed in significantly high concentrations in plasma ($p < 0.05$), compared to their lipomer analogues. Further drug-plasma kinetic analysis revealed C_{max} of 95.11, 87.40 and 74.00% for LTG, TX and LD, respectively. These were achieved at respective T_{max} of 8, 24 and 5 h, with the highest AUC reported for TX, followed by LTG; which were both significantly different from each other and from LD which had the min AUC value, ($p < 0.05$).

Analysis of brain homogenate, graphically presented in Fig. 9, indicate significantly higher C_{max} values of LTG, TX, LD from LF20, TF20 and LD20, ($p < 0.05$): 99.29, 99.33, and 85.93%, respectively, compared to their plasma analogues and oral standards. This was similarly confirmed with significantly higher respective AUC values, ($p < 0.05$). Although LTG *in-vivo* release from both Lamictal® and LF20 lipomer had the same T_{max} value; 48 h, the latter showed a significantly higher C_{max} and AUC. As for TX and LD; each showed higher T_{max}, C_{max} and AUC values compared to their oral analogues.

In general, results compiles with the *in-vitro* release kinetic profile previously presented, the intended efficient targeting of the optimized lipomers, and the pharmacokinetic data available on the marketed standard tablets. Furthermore; lipomers efficiency in sustained drug delivery and *in-vitro/in-vivo* stability reported in previous studies (Cheow and Hadinoto, 2011), agrees with the week-long sustainable release of drugs from LF20, TF20 and LDF20, in the present study.

Relevance of the *in-vitro* optimized lipomers structural advantages, achieved in this study earlier, to their *in-vivo* results can be highlighted though tracking its journey from administration to target site (Mustafa et al., 2013). Once IV administered, none of the drugs appeared in plasma, thanks to the carrier's lipid monolayer; that functions as drug-diffusion barrier, till BBB is reached (Mayur and Zaved, 2015); which is, in turn, facilitated due to the Tween®80, anchor-like action; causing Apo lipoproteins adsorption to lipomers surface, whose uptake by brain capillary endothelial cells becomes facilitated, via receptor-mediated endocytosis, as camouflaged lipoproteins, hence; transferring drug particles into brain interior though diffusion or transcytosis (Garcia-Garcia et al., 2005), increasing lipomers retention within brain blood capillaries, as they bind to endothelial cell lining, creating drug concentration gradient, thus; enhancing further drug transport across BBB by passive diffusion (Kreuter, 2012), while allowing further cellular accumulation governed by lipomers' optimized hydrodynamic size and PEG moiety (He et al., 2010). Furthermore, Tween®80 is believed to inhibit drug efflux transporters at the BBB; namely P-gp (P-glycoprotein); warranting an improved internalization of lipomers and their prolonged residence in brain (Chen and Liu, 2012). As per its surfactant nature, it can solubilize the endothelial cell membrane lipids, as well, causing subsequent membrane fluidization and destabilization, resulting in drug permeability enhancement though BBB, coupled with simultaneous opsonization prevention, and MPS circumvention (Wang et al., 2013).

Once endocytosed, lipomers tend to shed off their "stealth" corona upon acidification of late endosome or early lysosome (Modi et al., 2009), though slow sequential hydrolysis; proceeding for hours, of the bi-ester bond linking DSPE-PEG conjugate (Fang et al., 2010). Once in acidic pH, one of the bonds becomes protonated, i.e.; more electrophilic, triggering hydrolysis of the second ester bond, causing PEG molecule to shed, facilitating lipomers fusion with the endosomal membrane, enhancing its escape into the cytoplasm; where the hydrophobic polymeric core liquidates,
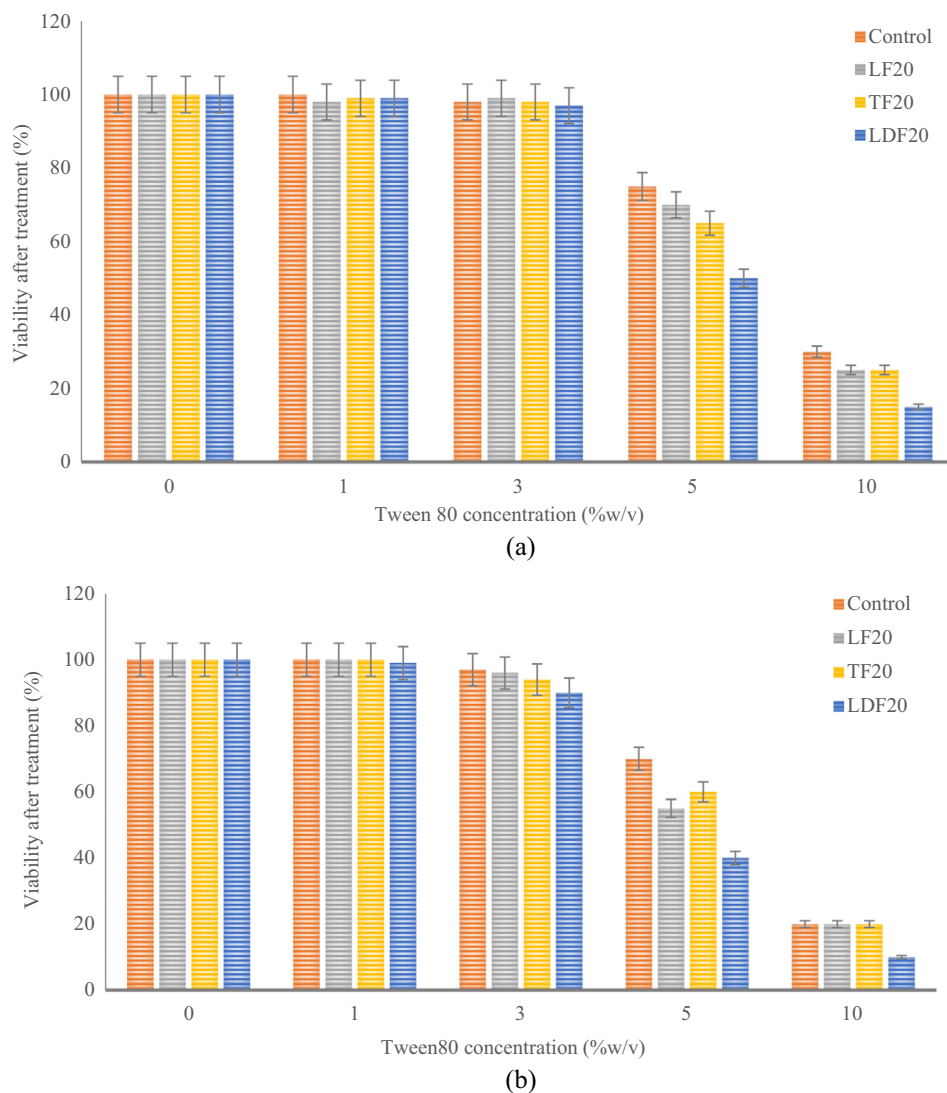
Fig. 7. Cytotoxicity of selected lipomers at increasing Tween®80 concentrations examined on (a) human brain cells and (b) blood brain barrier cells.

exposing the entrapped drug to diffusion (Yuba et al., 2010). This relatively long process would justify the observed high AUC, C_{max} and T_{max} values of lipomers; that were previously inferred from the *in-vitro* release profiles of each drug.

4.7. In-vitro/in-vivo correlation (IVIVC)

A credible IVIVC plays crucial role in development of pharmaceuticals; though building predictive mathematical models, (linear or non-linear), correlating an *in-vitro* property; rate or extent of drug release, of a dosage form to its *in-vivo* response; plasma drug concentration or amount absorbed, on assuming zero dissolution at time zero and complete dissolution at time t (Roudier et al., 2014).

As shown in Fig. 10, "Level A/point-to-point" IVIVC is selected, since it represents the highest category of correlation, in addition to its relevance to the *in-vitro* release method applied in this study (D'Souza et al., 2014). A linear correlation is observed for the three lipomer formulations: LF20, TF20 and LDF20 with R^2 values approaching unity and correlation coefficients of 0.93, 0.98, and 0.98, respectively, in the period from one to eight days. It is worth mentioning that; while a poor correlation was found with drug-plasma concentration, a very strong one was noted with drug-

brain concentration; which infers the brain as the main residence site of drugs encapsulated within lipomers, confirming its efficient targeting ability that was, as well, confirmed by the poor correlation in plasma.

4.8. In-vivo pharmacodynamic studies

4.8.1. Motor evaluation
4.8.1.1. Catalepsy assay. Catalepsy is a significant robust behavior mimicking symptoms of human extrapyramidal motor system disorders including inactivity and decreased responsiveness to stimuli, accompanied by tendency to maintain an immobile posture expressed though waxy flexibility of limbs, resulting, experimentally, in failure of animals to retain their normal posture in response to an externally imposed one. Generally, no specific mechanism has been defined as the ultimate one for catalepsy production. Hence; the present study would be investigating mechanisms governing catalepsy though use of LTG and TX, which are expected to display their anti-Parkinson's effect though mechanisms other than dopamine receptor activation. As recommended, control and standard groups were used to standardize empirical results obtained from neuro-pharmacological manipulation of neurotransmitters along the experiment (Sanberg et al., 1988).
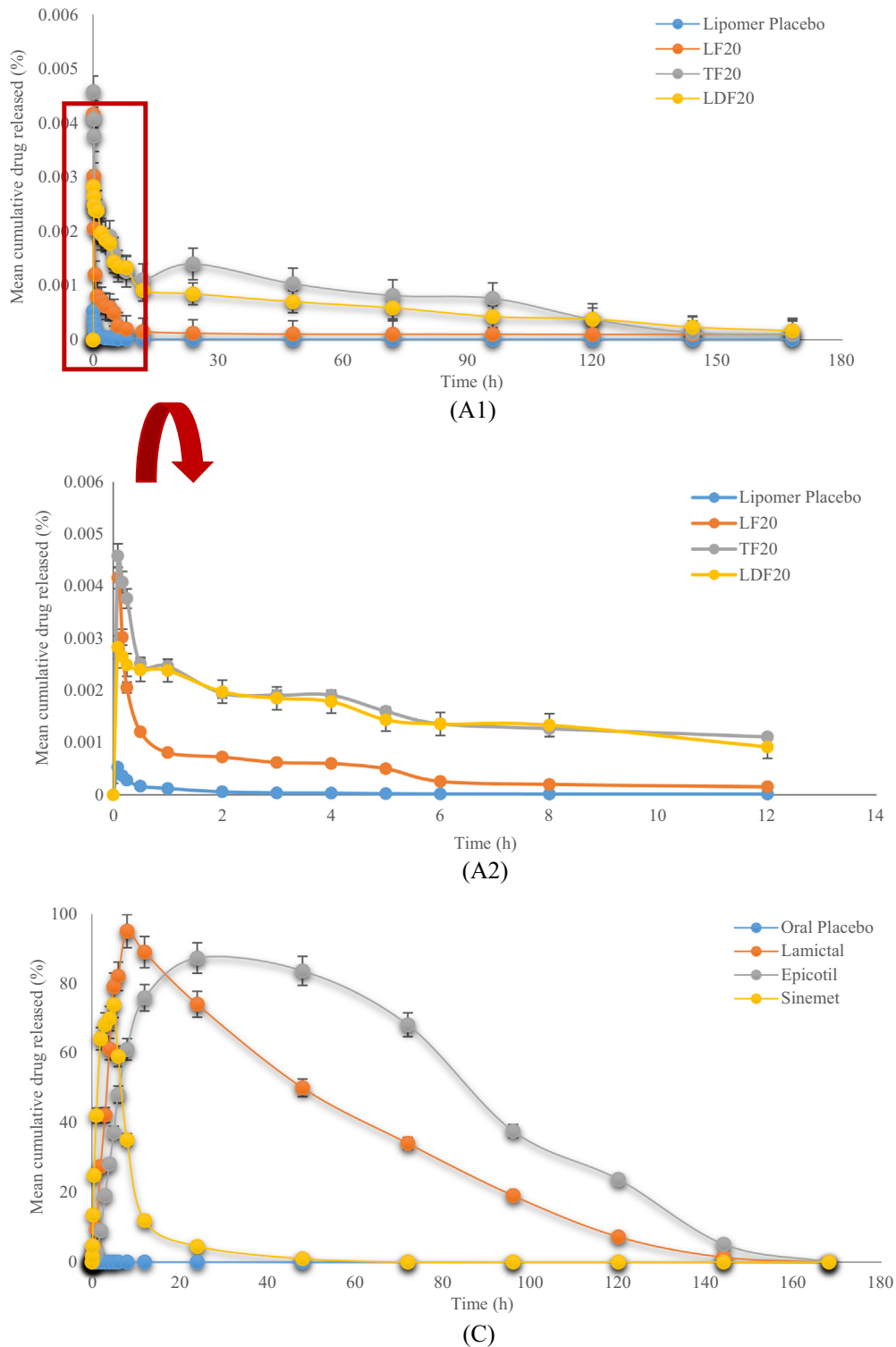
(A1)

(A2)

(C)

Fig. 8. Comparative mean cumulative drugs (LTG, TX, L-Dopa) released in rat plasma along a week time scale from (a) intravenous lipomers, (b) oral standard tablets.

From Table 6, positive control animals, retained their posture immediately due to absence of catalepsy inducing chemical: CPZ, or disease, while group 2 animals demonstrated highest cataleptic score (3.38 ± 0.23); since they received CPZ, with no treatment. Generally, all treated groups (groups 3–9), showed a significantly low catalepsy score, ($p < 0.05$), compared to negative control; attributed to the anti-Parkinson's effect of each of the administered drugs in their variable dosage forms, counteracting the CPZ cata-

lepsy induction. In detail; it is noticed that the three standard drugs-receiving groups showed significantly higher cataleptic scores, ($p < 0.05$), compared to their corresponding IV-lipomers in the following significantly different, ($p < 0.05$), order: Epicotil® > Lamictal® > Sinemet®; 2.38 ± 0.35 > 1.19 ± 0.26 > 0.63 ± 0.23, respectively. Referring to the corresponding lipomer-receiving groups; the same significantly different score order, ($p < 0.05$), was kept as their oral standard counterparts; TF20 > LF20 > LDF20,
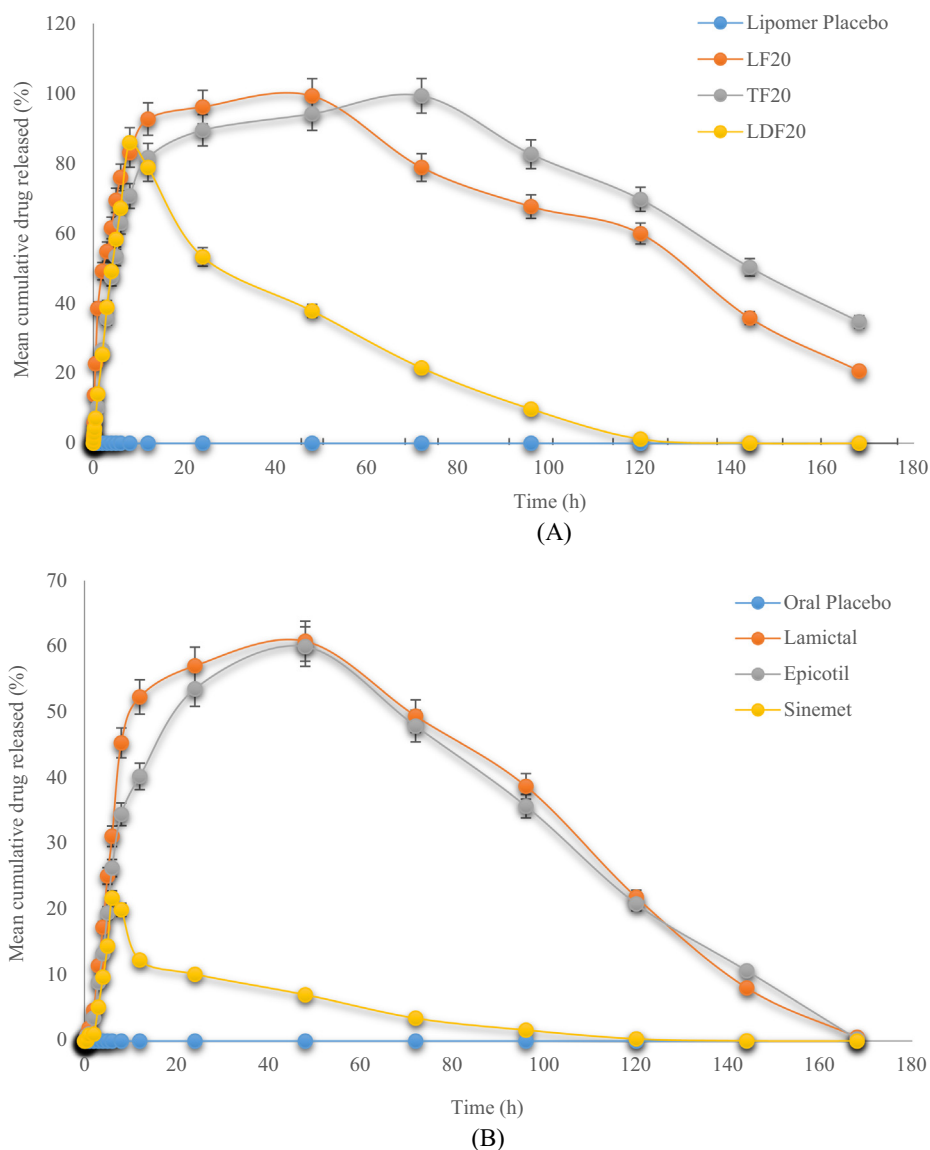
Fig. 9. Comparative mean cumulative drugs (LTG, TX, L-Dopa) released in rat brain homogenate along a week time scale from (a) intravenous lipomers, (b) oral standard tablets.

as follows: $1.39 \pm 0.33 > 0.67 \pm 0.25 > 0.08 \pm 0.18$, respectively. Finally, animals receiving combined LF20/TF20 IV lipomers totally reversed the cataleptic effect, showing "zero" catalepsy score; which is significantly low, ($p < 0.05$), compared to the other oral and IV lipomers, as well as CPZ-receiving group, and insignificantly different from positive control, ($p \geq 0.05$); suggesting a synergistic effect that is significantly effective compared to L-Dopa tablet and lipomers; based on combining LTG and TX different mechanisms of actions.

4.8.1.2. Open field activity. From results presented in Table 6, effect of CPZ administration in induction of Parkinsonism was reflected though a significantly deteriorated motor activity in negative control group ($p < 0.05$), compared to positive control; 7.88 ± 1.17 *vs.* 98.06 ± 5.71 cm crossed in open field, respectively. Rats in all standard groups showed significantly higher motor activity compared to negative control; which was simultaneously significantly lower compared to positive control, $p < 0.05$. An inter-group significant difference in rats' locomotor activity was also reported among the three standard groups, $p < 0.05$: Sinemet® (60.63 ± 4.30)

cm > Lamictal® (41.75 ± 3.94) cm > Epicotil® (25.11 ± 2.68) cm. On comparing standard to their corresponding IV groups, a significantly improved motor activity was observed in the latter; with similar orderly significant difference, $p < 0.05$: LDF20 (89.22 ± 5.83) cm > LF20 (72.56 ± 5.73) cm > TF20 (39.89 ± 4.15) cm. Finally; animals receiving combined LF20/TF20 lipomers showed a significantly improved motor activity; 86.78 ± 6.44 cm; the highest, $p < 0.05$, compared to all experimental groups with the exception of LDF20; where difference was non-significant, $p \geq 0.05$.

4.8.1.3. Grip strength "Wire-hanging" assay. From Table 6, data reflected mean time taken by rats of each group to keep grip of the stainless steel bar; inferring grip strength and muscular tone that is directly proportional to time recorded. It is clear that CPZ administration significantly deteriorated rats' muscular tone, ($p < 0.05$), compared to other experimental groups, with hanging time of 3.66 ± 0.82 s. Whereas; IV administration of LTG, TX and L-Dopa lipomers significantly improved muscular toning compared to their corresponding oral standard tablets, ($p < 0.05$):
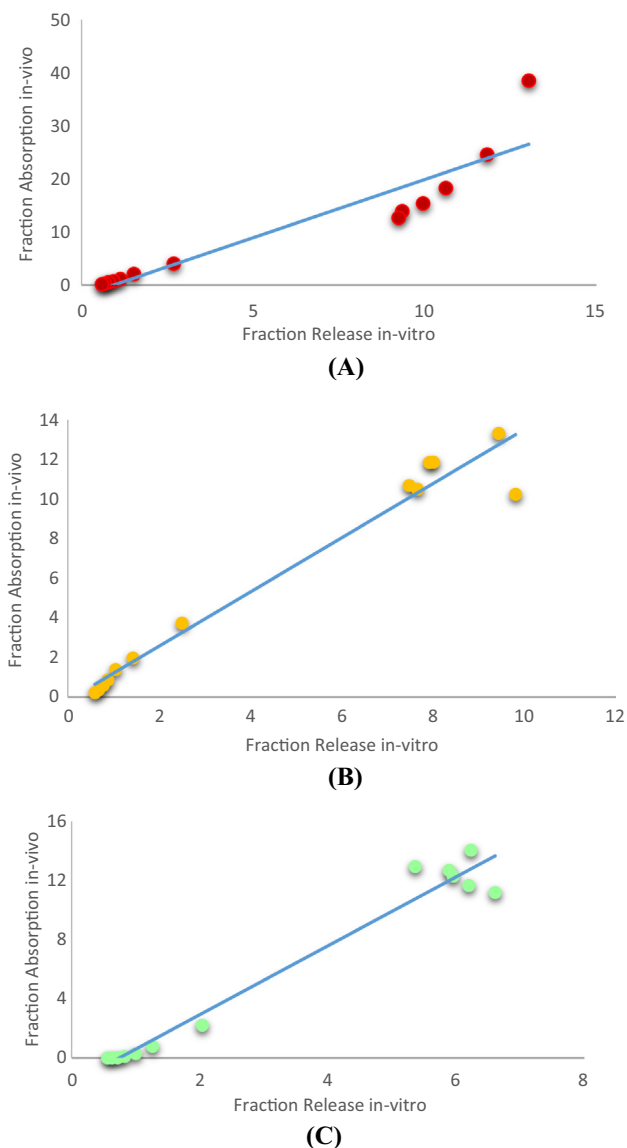
Fig. 10. Level A IVIVC between in and vitro release profiles and in-vivo absorption data of various lipomer formulations (a) lamotrigine, (b) tenoxicam, (c) L-dopa.

nigra and decreasing monoamine levels at nerve terminals (Naeem et al., 2017).

A number of mechanisms have been suggested, along literature, for clarifying LTG effect on improving locomotor activity and reversing catalepsy, with no concrete evidence of the prevalence of any over the others. Primarily; its long-term administration is thought to boost dopamine release in significantly high levels (Ahmad et al., 2004); directly, though weak binding to dopamine D1/D2 receptors, and indirectly, though serotonergic modulation of dopaminergic transmission; though inhibition of serotonin reuptake; enhancing serotonergic transmission with subsequent increase in dopamine levels (Dibue-Adjei et al., 2017). Furthermore; LTG is believed to weakly bind to GABA receptors; that regulates dopamine-mediated actions in extrapyramidal system, and finally, an anti-glutamatergic effect of LTG was reported in literature, as well (Ramadan et al., 2012).

Referring to TX neuroprotective action; reflected though its anti-cataleptic effect, ameliorated motor activity in open field test, and better muscular coordination in grip strength test, this can be explained though improving neurotransmission by raising dopamine levels in basal ganglia, which is responsible for hyper locomotion and muscular strength (Kaizaki et al., 2013), in addition to its inhibitory effect on cyclooxygenase "COX" enzymes, predominantly localized in microglia; resulting in subsequent inhibition of cytokines production (IL-1β and TNFα), and prostaglandin up-regulation (Ambhore et al., 2012) within the brain.

4.8.2. Cognitive evaluation

4.8.2.1. Water maze memory assay. **Assessment of short term memory (STM) and learning** showed that CPZ lead to significant increase in mean escape latency time ($p < 0.05$); with rats consuming maximum time of 83.25 ± 6.78 s to reach the platform, compared to 11.22 ± 3.07 s taken by placebo rats to reach the same point, and to both standard and test groups; whose escape latency period significantly decreased, $p < 0.05$, in the following order: 69.63 ± 5.60 s (Epicotil®) > 51.13 ± 5.89 s (Lamictal®) > 33.63 ± 2.35 s (Sinemet®), as standard drugs, and 39.22 ± 3.21 s (TF20) > 30.56 ± 4.02 s (LF20) > 20.96 ± 2.15 s (LDF20), as lipomers. It is worth noting that all test groups showed significantly lower escape latency time compared to their corresponding oral standards, $p < 0.05$. Furthermore, administration of the combined LF20/TF20 lipomers resulted in significant decrease in latency time compared to all groups; 14.01 ± 3.13 s, with the exception of placebo rats.

On assessing long term memory, no significant difference was observed in escape latency period in both positive and negative control rats, $p \geq 0.05$. Further on; a significant increase in latency time was observed after 24 h of Sinemet® administration compared to its 1 h reported reading. This might be primarily attributed to drug elimination as per its very short biological half-life, however; such observed increase was still significantly lower, $p < 0.05$, than negative control; which might be attributed to the learning curve effect that increased along the 24 h duration. Same effect can also justify the insignificant changes in escape latency time of both Lamictal® and Epicotil®, compared to the previous day readings. In addition; both drugs have long biological half-lives exceeding 24 h, together with high protein binding tendency. Thereby; the decrease in LTG or TX levels in blood after 24 h was compensated by the increase in rats' learning curve leading to non-significant changes in the resulting latency period.

Finally, an additive effect of learning curve increase and the increase in amount of drug released from the tested lipomers, resulted in significant decrease, $p < 0.05$, in latency period compared to their STM readings, in the same order: 31.08 ± 2.72 s (Epicotil®) > 21.42 ± 3.59 s (Lamictal®) > 13.74 ± 2.43 s (Sinemet®),

(156.67 ± 6.58 *vs.* 112.25 ± 4.92), (130.11 ± 5.13 *vs.* 80.88 ± 7.32), and (202.44 ± 9.62 *vs.* 139.25 ± 12.20) s, respectively, with L-Dopa demonstrating the most significant, ($p < 0.05$), effect followed by LTG then TX, in each of the tested delivery systems independently. Finally, combined LF20/TX20 lipomers improved muscular tone and grip strength in rats in the most significant manner, $p < 0.05$, compared to all other formulations; both standard and test; with hanging time of 253.67 ± 6.98 s achieved.

Briefly; from previous results evaluating locomotor activity; it is clear that LTG, TX and L-Dopa, each manifest its anti-Parkinson's effect though a different mechanism. Along literature; catalepsy and other locomotor impairment; weak muscular coordination and grip strength, have been correlated to blockage of dopamine receptors; creating positive relation between decrease in striatal dopamine and cataleptic intensity of anti-dopaminergic drugs (Vadlamudi et al., 2016), inferring the controversial effect of both CPZ-induction and L-Dopa inhibition of locomotor impairment; where the former develops motor deterioration in the form of hypolocomotion, passivity and muscular rigidity in Parkinson's animal models though blocking dopamine receptors in substantia

Table 6
In-vivo behavioral pharmacodynamic assessment of anti-Parkinson's effect of selected lipomers and their corresponding standards.

Group		Treatment	Motor activity evaluation (Mean values ± SD)			Cognitive assay (Mean values ± SD)		
			Catalepsy Score	Open Field Distance crossed (cm)	Grip Strength Time (s)	Water Maze Escape Latency Time (sec)		Passive Avoidance Latency Time (s)
						STM[*]	LTM[*]	
1	Positive control	IV Placebo	0.00 ± 0.00	98.06 ± 5.71	279.67 ± 9.89	11.22 ± 3.07	12.58 ± 4.13	151.46 ± 7.91
2	Negative control	IP CPZ	3.38 ± 0.23	7.88 ± 1.17	3.66 ± 0.82	83.25 ± 6.78	87.52 ± 5.60	18.54 ± 3.73
3	Standard LTG	Oral Lamictal®	1.19 ± 0.26	41.75 ± 3.94	112.25 ± 4.92	51.13 ± 5.89	54.33 ± 3.97	57.48 ± 4.16
4	Standard TX	Oral Epicotil®	2.38 ± 0.35	25.11 ± 2.68	80.88 ± 7.32	69.63 ± 5.60	72.61 ± 3.44	42.19 ± 5.49
5	Standard L-Dopa	Oral Sinemet®	0.63 ± 0.23	60.63 ± 4.30	139.25 ± 12.20	33.63 ± 2.35	49.13 ± 2.57	79.23 ± 5.75
6	LTG IV test	IV LF20	0.67 ± 0.25	72.56 ± 5.73	156.67 ± 6.58	30.56 ± 4.02	21.42 ± 3.59	84.29 ± 6.02
7	TX IV test	IV TF20	1.39 ± 0.33	39.89 ± 4.15	130.11 ± 5.13	39.22 ± 3.21	31.08 ± 2.72	73.23 ± 5.99
8	L-Dopa IV test	IV LDF20	0.08 ± 0.18	89.22 ± 5.83	202.44 ± 9.62	20.96 ± 2.15	13.74 ± 2.43	107.31 ± 8.87
9	Combined IV test	IV "LF20/TF20"	0.00 ± 0.00	86.78 ± 6.44	253.67 ± 6.98	14.01 ± 3.13	13.21 ± 3.30	135.16 ± 9.56

[*] STM: short-term memory, LTM: Long-term memory.

moreover; no significant difference was noticed between the latter and the combined LF20/TF20 lipomers, p ≥ 0.05.

4.8.2.2. Passive avoidance test. Escape latency, presented in Table 6, is calculated as time a rat spends in the illuminated safe box, before it returns again to the dark one. Negative control showed passive attitude though a significantly decreased escape latency time of 18.54 ± 3.73 s, compared to other experimental groups, p < 0.05. On receiving various oral standard drugs, a significantly improved escape latency time was observed in the following significantly different order in seconds, p < 0.05: 42.19 ± 5.49 (Epicotil®) < 57.48 ± 4.16 (Lamictal®) < 79.23 ± 5.75 (Sinemet®). It is worth noting that all IV lipomers improved latency in a more significant manner compared to their corresponding oral standards, following the same significant order in sec, p < 0.05: 73.23 ± 5.99 (TF20) < 84.29 ± 6.02 (LF20) < 107.31 ± 8.875 (LDF20). The combined LF20/TF20 lipomers showed a highly significant latency time, p < 0.05, inferring the best drug activity, compared to test, standard and negative control groups.

Induction of PD using CPZ along 21 days, resulted in impaired memory and learning, reflected though relatively fast entry of rats in punishment box, which comes in accordance with a previous study carried by Johansson et al., who attributed similar results to free radical formation ability of CPZ, yielding damage in dopaminergic cells, reducing epinephrine and serotonin concentration; resulting in amnesia and learning deficiency (Johansson et al., 2012). Long-term potentiation (LTP) is one of the major cellular mechanisms involved in learning and memory; where the latter is thought to be encoded by modification of synaptic strength; manifested though long-lasting enhancement in signal transmission between two neurons resulting from their synchronous stimulation. In detail; LTP is regulated via reactive oxygen species

(ROS); positively though glutamate receptors activation, resulting in calcium influx, activating different kinases, facilitating its formation, and negatively though controlling phosphatases; where superoxide anion radical ($O_2^{\bullet-}$) accumulates following glutamate receptors activation, though conversion of NADPH oxidase (Kyle et al., 2013). Such glutamatergic hyperactivity promotes alteration in neurotransmitters in direct and indirect nigro-striatal pathways in Parkinson's patients; yielding excitotoxicity that contributes to neurodegenerative processes on one hand, and to pathophysiology of dyskinesia and motor fluctuations associated with chronic use of L-DOPA, on the other hand (Carrillo-Mora and Silva-Adaya, 2013).

Administration of TX, either orally or IV, significantly reverted such amnesiac behavior, providing better memory and learning performance, via inhibition of COX pathway and inflammatory cytokines which reduce oxidative stress and ultimately restore dopamine levels (Ambhore et al., 2012). Lamotrigine is thought to improve learning and memory though several mechanisms, including inhibition of voltage-dependent sodium, calcium and potassium channels; this is thought to decrease glutamate release, and inhibition of serotonin reuptake (pharmacological, xxxx). In addition; as an AMPA receptor positive allosteric potentiator, LTG administration would result in cognitive enhancement (Bobula and Hess, 2008)though interference with glutamatergic neurotransmission. Moreover; it blocks glutamate receptors including N-methyl-D-aspartate (NMDA), resulting in arachidonic acid (AA) cascade markers down regulation (Azadmanesh and Borgstahl, 2018), since NMDA receptors are responsible for AA signaling initiation in rat brain though controlling entry of extracellular calcium into the cell, stimulating calcium dependent cytosolic phospholipase A2 (cPLA2) to release AA from membrane phospholipid, which is then converted to pro-inflammatory PGE2 via membrane PGE synthase, consequently; yielding reduced brain COX

Table 7
In-vivo biochemical pharmacodynamic assessment of anti-Parkinson's effect of selected lipomers and their corresponding standards.

Group		Treatment	TBARS	GSH	Nitrite	Superoxide Dismutase Mean (nM/mgTP[*]) ± SD	Catalase (mmol/L/mg H_2O_2 degraded/min)
			Mean values(nmol/L/mg protein) ± SD				
1	Positive control	IV Placebo	20.91 ± 0.53	21.32 ± 0.41	3.08 ± 0.31	9.65 ± 0.07	117.69 ± 0.51
2	Negative control	IP CPZ	56.76 ± 0.82	3.55 ± 0.29	22.19 ± 0.55	28.37 ± 0.18	69.27 ± 0.38
3	Standard LTG	Oral Lamictal®	38.47 ± 0.91	13.57 ± 0.84	14.11 ± 0.36	14.92 ± 0.10	80.15 ± 0.88
4	Standard TX	Oral Epicotil®	35.15 ± 0.78	15.80 ± 1.02	10.82 ± 0.54	15.73 ± 0.09	*86.63 ± 0.49
5	Standard L-Dopa	Oral Sinemet®	40.12 ± 1.04	14.63 ± 0.71	12.63 ± 0.78	17.12 ± 0.04	91.42 ± 0.96
6	LTG IV test	IV LF20	32.49 ± 0.83	16.95 ± 0.68	8.14 ± 0.27	11.98 ± 0.09	105.18 ± 0.23
7	TX IV test	IV TF20	25.11 ± 0.65	18.24 ± 0.32	5.03 ± 0.41	11.03 ± 0.05	110.52 ± 0.42
8	L-Dopa IV test	IV LDF20	29.36 ± 0.48	17.78 ± 0.25	6.17 ± 0.39	12.02 ± 0.08	114.70 ± 0.36
9	Combined IV test	IV "LF20/TF20"	21.16 ± 0.79	20.93 ± 0.43	3.65 ± 0.34	9.77 ± 0.06	117.32 ± 0.64

[*] TP = Total Protein.

activity, prostaglandin PGE2 concentration, and DNA binding of COX-2 transcription factor NF-κB (Kim et al., 2011).

4.8.3. Biochemical assays

4.8.3.1. Lipid peroxidation assay.
Lipid peroxidation is a biologically important free radical reaction, which result in peroxidative injury to plasma phospholipids, leading to severe cellular damage, unless reversed by efficient antioxidant. High rate of oxidative metabolism, coupled with low antioxidant defense and elevated polyunsaturated fatty acid levels, put the brain at high risk of free radical damage (Devi et al., 2008).

From Table 7; negative control rats showed significantly ($p < 0.05$), the highest TBARS value, as a result of non-treated CPZ-PD induction: 56.76 ± 0.82 (nmol/L/mg protein), compared to other experimental and positive control groups, with the latter showing, significantly ($p < 0.05$), the lowest TBARS value: 20.91 ± 0.53 (nmol/L/mg protein). Oral and IV administration of standard and test drugs, generally, resulted in significant reduction in TBARS ($p < 0.05$), reflecting their anti-PD effect, with the latter demonstrating a significantly better effect inferred from significantly lower TBARS values, compared to their corresponding standard oral formulations ($p < 0.05$), in the following TBARS descending order: L-Dopa > LTG > TX. This reflects the significantly high anti-oxidant effect of TX, ($p < 0.05$), compared to other drugs. Combining LTG and TX in IV lipomers, administered to group 9 showed the lowest TBARS value: 21.16 ± 0.97 (nmol/L/mg protein), that was insignificantly different from positive control and significantly different from all other groups at $p = 0.05$, indicating its efficiency in restoring peroxides and antioxidant levels to their normal values in rat brain.

4.8.3.2. Reduced glutathione (GSH).
Results presented in Table 7 show a significant reduction in GSH levels on administration of CPZ in group 2, ($p < 0.05$): 3.55 ± 0.29 (nmol/L/mg protein), compared to positive control: 21.32 ± 0.41 (nmol/L/mg protein). On one hand, in groups receiving oral standards; GSH values significantly increased, ($p < 0.05$), compared to group 2, in the following order: Epicotil® (15.80 ± 1.02) > Sinemet® (14.63 ± 0.71) > Lamictal® (13.57 ± 0.84) nmol/L/mg protein, with no significant difference observed between Lamictal® and Sinemet®, ($p \geq 0.05$). On the other hand, further increase in GSH values was observed on administration of IV lipomers, according to the following order: LF20/TF20 (20.93 ± 0.43) > TF20 (18.24 ± 0.32) > LDF20 (17.78 ± 0.25) > LF20 (16.95 ± 0.68) nmol/L/mg protein, with the former showing the most significant effect ($p < 0.05$); approaching normal compared to positive control ($p \geq 0.05$).

4.8.3.3. Nitrite levels.
Parkinson's patients generally suffer increased cerebral oxidative-stress that yields nitric oxide; which then oxidizes spontaneously into nitrite and nitrate. As shown in Table 7; group 2 rats showed the highest nitrite levels, which are significantly different from all other groups, ($p < 0.05$): 22.19 ± 0.55 nmol/L/mg protein. Administration of anti-PD drugs either orally or IV lead to significant decrease in nitrite levels, with the latter showing better efficiency, inferred from its significantly lower nitrite levels measured, ($p < 0.05$): 8.14 ± 0.27 vs. 14.11 ± 0.36, 5.03 ± 0.41 vs. 10.82 ± 0.54, and 6.17 ± 0.39 vs. 12.63 ± 0.78 nmol/L/mg protein, for LF20 vs. Lamictal®, TF20 vs. Epicotil®, and LDF20 vs. Sinemet®, respectively, noting that IV lipomers were as twice effective as their oral counterparts. It is also clear that L-Dopa, in its either forms, was significantly the most effective, followed by TX, then LTG, ($p < 0.05$). Finally, combinant LF20/TF20 lipomers manifested an additive effect, resulting in significant reduction in nitrite levels, ($p < 0.05$), compared to other formulations, which was, however; insignificantly different from positive control, ($p \geq 0.05$): 3.65 ± 0.34 vs. 3.08 ± 0.31 3.08 ± 0.31, for LF20/TF20 vs. Placebo.

4.8.3.4. Catalase levels.
On reviewing Table 7, it was observed that rats receiving CPZ showed a significantly low mean catalase level, $p < 0.05$: 69.27 ± 0.38 mmol/L/mgH2O2 degraded/min, compared to other experimental groups and positive control; showing significantly high mean values, $p < 0.05$: 117.69 ± 0.51 mmol/L/mg H2O2 degraded/min. Administration of oral Sinemet®, Epicotil® and Lamictal®, resulted in a significant increase in mean catalase levels, $p < 0.05$: 91.42 ± 0.96, 86.63 ± 0.49 and 80.15 ± 0.88 mmol/L/mg H2O2 degraded/min, respectively, with the former showing the highest anti-oxidant effect. Administration of the same drugs in their IV lipomer form lead to further significant increase in mean catalase levels, $p < 0.05$, in the same order, compared to their oral counterparts: 114.70 ± 0.36, 110.52 ± 0.42 and 105.18 ± 0.23 mmol/L/mg H2O2 degraded/min, respectively for LDF20, TF20 and LF20. As for the combined LF20/TF20 lipomer formulation, a mean catalase level of 117.32 ± 0.64 mmol/L/mg H2O2 degraded/min was obtained, which is significantly high compared to all other formulations ($p < 0.05$), and non-significantly different from positive control, ($p \geq 0.05$).

4.8.3.5. Superoxide dismutase activity.
Extracellular SOD represents a major defense system against superoxide, being a target for oxidative damage (Azadmanesh and Borgstahl, 2018). Results listed in Table 7 show that induction of PD in group 2 lead to increase in SOD enzyme production in rat brain: 28.37 ± 0.18 nM/mg TP, which is significantly the highest value obtained, compared to the remaining experimental groups, which were, on the other side, compared to positive control showing the minimum, significantly different, value for SOD: 9.65 ± 0.07 nM/mg TP, ($p < 0.05$). Both oral and IV administered drugs had a significant effect on lowering SOD levels, with the latter showing better efficiency, reflected though significantly lower SOD values on comparing each IV drug to its corresponding oral standard, ($p < 0.05$). Combining both LTG and TX in one IV lipomer formulation resulted in an additive significant reduction in SOD levels ($p < 0.05$), compared to other groups, however, it was non-significantly different from positive control, ($p \geq 0.05$).

Oxidative stress augmentation is one of PD neuropathophysiological key characteristics; taking place though free radical generation (Bhimani, 2014). Biochemical assay results presented along this study, were found to be consistent with results of cognitive and behavioral assays, presented earlier. These could be linked though understanding oxidative stress; which contributes to several CNS physiological functions. In general, normal cells tend to generate ROS while limiting their over-accumulation though maintaining prooxidant/antioxidant balance via enzymatic and non-enzymatic antioxidant systems, as means of self-defense against cellular damage caused by oxidative stress; resulting from disturbance in the mentioned balance. As secondary messengers; ROS are involved in regulation of a number of cellular signaling pathways controlling cell survival, migration and proliferation (Vadlamudi et al., 2016).

Antioxidants generally perform their protective functions primarily though $O_2^{\bullet-}$ degeneration into non-radical hydrogen peroxide (H_2O_2); though various pathways. In the present study, antioxidants are represented though glutathione peroxidase (GPx), glutathione (GSH), nitric oxide synthase (NOS), SOD, and catalase (Valko et al., 2007); where SOD initially converts $O_2^{\bullet-}$ into H_2O_2, which, by turn, is converted to H_2O and O_2 via catalase. This latter conversion also occurs though glutathione buffer system; when GPx transforms peroxides: H_2O_2 and organic peroxide (ROOH), into H_2O in the presence of tripeptide glutathione (GSH); which reacts, in parallel, with radicals forming thiyl radi-

cals; that dimerize into a transient non-radical oxidized disulfide form (GSSG) that finally reduces to regenerate GSH by glutathione reductase (Stanley et al., 2011). Finally, reactive nitrogen intermediates (RNI) comprising different forms of nitric oxide ($NO^•$), nitroxyl anion (NO^-), nitrosonium cation (NO^+), and peroxynitrite ($ONOO^-$), are involved in regulation of apoptotic or necrotic cell death; where nitric oxide ($NO^•$) is enzymatically generated by NOS, to react, further, with O_2^- producing $ONOO^-$ (Massaad and Klann, 2011).

CPZ acts by increasing lipid peroxidation, free radical formation and decreasing glutathione reduction in brain (Sandhu and Rana, 2013). Generally, when glutathione levels decrease in brain, H_2O_2 clearance in basal ganglia becomes impaired; creating oxidative stress though formation of toxic hydroxyl radicals (Niehaus and Samuelson, 1968). This provides further insights about the improved cognitive abilities in water maze and passive avoidance tests, on administration of TX, L-Dopa and LTG, where each counteracted the CPZ-induced actions though reducing oxidative stress in hippocampus and amygdala, restoring both short term and long term memory, since PD-associated elevated levels of PGE2, TNFα and other cytokines would result in free radical production in rats hippocampus, altering the NMDA receptors action; previously discussed, impairing cognitive functions (Lau et al., 2009).

Furthermore; several studies hypothesized that LTG generates reactive moieties that can covalently bind to vital biomolecules, as proteins, lipids or DNA, protecting them against systemic toxicity, though inhibition of free radical production, eliciting oxidative damage. Moreover, LTG's capability of keeping "prooxidant/anti oxidant" balance in patients has been proved, in previous clinical studies, though controlling lipid peroxidation and free radical production processes via its antioxidant defense mechanisms (Varoglu et al., 2010). In addition; LTG metabolism takes place though glucuronidation, with minimal involvement of CYP-450 and parallel induction of antioxidant enzymes, with initial increase in SOD activity noticed; which was justified as either a probable sort of adaptive reaction to increased systemic oxidative stress or a consequent leakage from damaged tissues. Also, the persistent increase in antioxidant enzyme activities reported in literature after LTG administration, infers an up-regulation in antioxidant enzyme synthesis and consequent activities; which is perceived as a secondary phenomenon resulting enhanced CYP-450 free radical production. Briefly; the overall decrease in oxidative damage indicates a positive effect of LTG on the prooxidant/antioxidant balance though normalization of oxidative stress byproducts (Panayiotopoulos, 2010).

Tenoxicam was also thought to improve neurotransmission, though raising monoamines, dopamine and glutathione levels in basal ganglia; where high dopamine levels control hyper locomotion and muscular strength (Johansson et al., 2012), in addition to its reported reduction of oxidative stress though inhibition of induced nitric oxide synthase (iNOS), ROS, and any consequent prostanoids mediated neuroinflammation while decreasing TPAR (Schwartz and Shechter, 2010).

5. Conclusion

Facilitated BBB passage of fusogenic lipomers of DSPE-PEG conjugate was proved pharmacokinetically and dynamically, through fusing with cellular or endosomal membranes at the target site. Briefly; "(lipid/PEG):Polymer" weight ratio of (1:9) and (1:4) yielded spherical, double layered HNPs of estimated PS < 200 nm, narrow range PDI (between 0.1 and 0.2), and highly negative ZP, inferring system's homogeneity, stability, circulation time prolongation, BBB targeting and residence efficiency. Drug loading generally increased on increasing drug and/or lipid content, however,

increasing polymeric content had no effect. The EE increased as function of increasing polymer content too.

The F20 lipomer of ["lecithin/PEG":PLCL] ratio of 1:9, (drug:polymer) ratio of 5:1, and (lecithin:PEG) ratio of 4:1, showed superior optimized properties, with proved stability and biocompatibility at the employed concentrations, and a very strong IVIVC point to point linear correlation with drug-brain concentration; inferring brain as their main residence site. Generally; pharmacodynamic profile of all lipomers was significantly more efficient compared to their corresponding oral marketed Sinemet® (L-Dopa & Carbidopa); in both biological and biochemical assays. Combined "LF20/TF20" lipomers was the most efficient anti-PD; suggesting higher efficiency in improving Parkinson's patients overall health state on long-term treatment. Thus; the proposed hypothesis was fulfilled and experimentally proven with new prescription profile for both LTG and TX.

References

A pharmacological overview of lamotrigine for the treatment of epilepsy..

Agarwal, A., Kale, R.K., 2001. Radiation induced peroxidative damage: mechanism and significance. Ind. J. Exp. Biol. 39, 291–309.

Ahmad, N., 2017. Rasagiline-encapsulated chitosan-coated PLGA nanoparticles targeted to the brain in the treatment of Parkinson's disease. J. Liq. Chromatogr. Relat. Technol. 40 (13), 677–690.

Ahmad, N., Ahmad, R., Alam, M., Ahmad, F., 2018a. Quantification and brain targeting of Eugenol-loaded surface modified nanoparticles through intranasal route in the treatment of cerebral ischemia. Drug Res. 68 (10), 584–595.

Ahmad, N., Ahmad, R., Alam, M.A., Ahmad, F.J., Amir, M., 2018b. Impact of ultrasonication techniques on the preparation of novel Amiloride-nanoemulsion used for intranasal delivery in the treatment of epilepsy. Artif. Cells Nanomed. Biotechnol. 46 (sup3), S192–S207.

Ahmad, N., Al-Subaie, A.M., Ahmad, R., Sharma, S., Alam, M.A., Ashafaq, M., Rub, R.A., Ahmad, F.J., 2019. Brain-targeted glycyrrhizic-acid-loaded surface decorated nanoparticles for treatment of cerebral ischaemia and its toxicity assessment. Artif. Cells Nanomed. Biotechnol. 47 (1), 475–490.

Ahmad, Sh., Fowler, L.J., Whitton, P.S., 2004. Effect of acute and chronic lamotrigine on basal and stimulated extracellular 5-hydroxytryptamine and dopamine in the hippocampus of the freely moving rat. Br. J. Pharmacol. 142, 136–142.

Ahmed, F., Ali, M.J., Kondapi, A.K., 2014. Carboplatin loaded protein nanoparticles exhibit improve anti-proliferative activity in retinoblastoma cells. Int. J. Biol. Macromol. 70, 572–582.

Alexis, F., Pridgen, E., Molnar, L.K., Farokhzad, O.C., 2008. Factors affecting the clearance and biodistribution of polymeric nanoparticles. Mol. Pharm. 5 (4), 505–515.

Ambhore, N., Antony, S., Mali, J., Kanhed, A., Bhalerao, A., Bhojraj, S., 2012. Pharmacological and biochemical interventions of cigarette smoke, alcohol, and sexual mating frequency on idiopathic rat model of Parkinson's disease. J. Young Pharm. 4 (3), 177–183.

Ammar, H.O., Ghorab, M.M., Mahmoud, A.A., Higazy, I.M., 2018. Lamotrigine loaded poly-ε-(d, l-lactide-co-caprolactone) nanoparticles as brain delivery system. Eur. J. Pharm. Sci. 115, 77–87.

Aryal, S., Hu, C.M., Zhang, L., 2010. Polymer-cisplatin conjugate nanoparticles fir acid-responsive drug delivery. ACS Nano 4 (1), 251–258.

Azadmanesh, J., Borgstah, G.E.O., 2018. A review of the catalytic mechanism of human manganese superoxide dismutase. Antioxidants 7 (25). https://doi.org/10.3390/antiox7020025.

Badran, M.M., Mady, M.M., Ghannam, M.M., Shakeel, F., 2017. Preparation and characterization of polymeric nanoparticles surface modified with chitosan for target treatment of colorectal cancer. Int. J. Biol. Macromol. 95, 643–649.

Bahuguna, A., Khan, I., Bajpai, V.K., 2017. Kang S-Ch. MTT assay to evaluate the cytotoxic potential of a drug. Bangladesh. J. Pharmacol. 12, 115–118.

Bãnez-Coronel, M., De Molina, A.R., Rodríguez-González, A., Sarmentero, J., Ramos, M.A., Garcia-Cabezas, M.A., Garcia-Oroz, L., Lacal, J.C., 2008. Choline kinase alpha depletion selectively kills tumoral cells. Curr. Cancer Drug Targets 8 (8), 709–719.

Barltrop, J.A., Owen, T.C., Cory, A.H., Cory, J.G., 1991. 5-(3-carboxymethoxyphenyl)-2- (4,5-dimethylthiazoly)-3-(4-sulfophenyl) tetrazolium, inner salt (MTS) and related analogs of 3-(4,5-dimethylthiazolyl)-2,5-diphenyltetrazolium bromide (MTT) reducing to purple water soluble formazans as cell-viability indicators. Bioorg. Med. Chem. Lett. 1 (11), 611–614.

Bassani, T.B., Vital, M.A., Rauh, L.K., 2015. Neuroinflammation in the pathophysiology of Parkinson's disease and therapeutic evidence of anti-inflammatory drugs. Arq. Neuropsiquatr. 73 (7), 616–623.

Bence, A.K., Worthen, D.R., Stables, J.P., Crooks, P.A., 2003. An in vivo evaluation of the antiseizure activity and acute neurotoxicity of agmatine. J. Pharmacol. Biochem. Behav. 74, 771–775.

Bender, E.A., Adorne, M.D., Colome, L.M., Abdalla, D.S., Guterres, S.S., Pohlmann, A.R., 2012. Hemocompatibility of poly (ε-caprolactone) lipid-core nanocapsules

stabilized with polysorbate80-lecithin and uncoated or coated with chitosan. Int. J. Pharm. 426 (1–2), 271–279.

Bhimani, R., 2014. Understanding the burden on caregivers of people with Parkinson's: a scoping review of the literature. Rehabil Res Pract 2014, 718527.

Bishnoi, M., Chopra, K., Kulkarni, S.K., 2006. Involvement of adenosinergic receptor system in an animal model of tardive dyskinesia and associated behavioural, biochemical and neurochemical changes. Eur. J. Pharmacol. 552, 55–66.

Bobula, B., Hess, G., 2008. Antidepressant treatments-induced modifications of glutamatergic transmission in rat frontal cortex. Pharmacol. Rep. 60 (6), 865–871.

Brooks, D.J., 2008. Optimizing levodopa therapy for Parkinson's disease with levodopa /carbidopa /entacapone: implications from a clinical and patient perspective. Neuropsychiatr. Dis. Treat. 4, 39–47.

Carrillo-Mora, P., Silva-Adaya, D., 2013. Villasenõr-Aguayo K Glutamate in Parkinson's disease: role of antiglutamatergic drugs. Basal Ganglia 3, 147–157.

Castel-Branco, M.M., Almeida, A.M., Falcão, A.C., Macedo, T.A., Caramona, M.M., Lopez, F.G., 2001. Lamotrigine analysis in blood and brain by high-performance liquid chromatography. J. Chromatogr. B Biomed. Sci. Appl. 755 (1–2), 119–127.

CellTiter 96® Non-Radioactive Cell Proliferation Assay Technical Bulletin #TB112, Promega Corporation.

Chacko, B.J., Palanisamy, S., Gowrishankar, N.L., Honeypriya, J., Sumathy, A., 2018. Effect of surfactant coating on brain targeting polymeric nanoparticles: a review. Indian J. Pharm. Sci. 80 (2), 215–222.

Chan, J.M., Zhang, L., Yuet, K.P., Liao, G., Rhee, J.W., Langer, R., Farokhzad, O.C., 2009. PLGA-lecithin-PEG core-shell nanoparticles for controlled drug delivery. Biomaterials 30 (8), 1627–1634.

Chaudhuri, K.R., Odin, P., Antonini, A., Martinez-Martin, P., 2011. Parkinson's disease: the non-motor issues. Parkinsonism Relat. Disord. 17, 717–723.

Chen, Y.-Ch., Hsieh, W.-Y., Lee, W.-F., Zeng, D.-T., 2011. Effects of surface modification of PLGA-PEG-PLGA nanoparticles on loperamide delivery efficiency across the blood–brain barrier. J. Biomat. Appl. 27 (7), 909–922.

Chen, Y., Liu, L., 2012. Modern methods for delivery of drugs across the blood-brain barrier. Adv. Drug Deliv. Rev. 64 (7), 640–665.

Chen, H., Zhang, S.M., Hernan, M.A., Schwarzschild, M.A., Willett, W.C., Colditz, G.A., Speizer, F.E., Ascherio, A., 2003. Non-steroidal anti-inflammatory drugs and the risk of Parkinson disease. Arch. Neurol. 60, 1059–1064.

Cheng, G., Mi, L., Cao, Z., Xue, H., Yu, Q., Carr, L., Jiang, S., 2010. Functionalizable and ultrastable zwitterionic nanogels. Langmuir 26 (10), 6883–6886.

Cheow, W.S., Hadinoto, K., 2011. Factors affecting drug encapsulation and stability of lipid-polymer hybrid nanoparticles. Colloids Surf. B Biointerfaces 85 (2), 214–220.

De Miguel, I., Imbertie, L., Rieumajou, V., Major, M., Kravtzoff, R., Betbeder, D., 2000. Proofs of the structure of lipid coated nanoparticles (SMBV) used as drug carriers. Pharm. Res. 17, 817–824.

Devi, P.U., Manocha, A., Vohora, D., 2008. Seizures, antiepileptics, antioxidants and oxidative stress: an insight for re searchers. Expert Opin. Pharmacother. 9, 3169–3177.

Dibue-Adjei, M., Kamp, M.A., Alpdogan, S., Tevoufouet, E.E., Neiss, W.F., Hescheler, J., Schneider, T., 2017. Cav2.3 (R-Type) calcium channels are critical for mediating anticonvulsive and neuroprotective properties of lamotrigine in vivo. Cell. Physiol. Biochem. 44 (3), 935–947.

D'Souza, S., Faraj, J.A., Giovagnoli, S., Deluca, P.P., 2014. IVIVC from Long Acting Olanzapine Microspheres. Int. J. Biomater. https://doi.org/10.1155/2014/407065..

Ellman, G.L., 1959. Tissue sulfhydryl groups. Arch. Biochem. Biophys. 82, 70–77.

Etheridge, M.L., Campbell, S.A., Erdman, A.G., Haynes, C.L., Wolf, S.M., McCullough, J., 2013. The big picture on nanomedicine: the state of investigational and approved nanomedicine products. Nanomedicine 9, 1–14.

Fang, R.H., Aryal, S., Hu, C.M., Zhang, L., 2010. Quick synthesis of lipid-polymer hybrid nanoparticles with low polydispersity using a single-step sonication method. Langmuir 26 (22), 16958–16962.

Gajra, B., Dalwadi, Ch., Patel, R., 2015. Formulation and optimization of itraconazole polymeric lipid hybrid nanoparticles (Lipomer) using box behnken design. J. Pharm. Sci. 23 (3), 1–15.

Garcia-Garcia, E., Andrieux, K., Gil, S., Couvreur, P., 2005. Colloidal carriers and blood-brain barrier (BBB) translocation: a way to deliver drugs to the brain?. Int. J. Pharm. 298 (2), 274–292.

Gonzalez-Carter, D.A., Ong, Z.Y., McGilvery, C.M., Dunlop, I.E., Dexter, D.T., Porter, A. E., 2019. L-DOPA functionalized, multi-branched gold nanoparticles as brain-targeted nano-vehicles. Nanomed. Nanotechnol. Biol. Med. 15, 1–11.

Gu, F., Zhang, L., Teply, B.A., Mann, N., Wang, A., Radovic-Moreno, A.F., Langer, R., Farokhzad, O.C., 2008. Precise engineering of targeted nanoparticles by using self-assembled biointegrated block copolymers. Proc. Natl. Acad. Sci. 105, 2586–2591.

Gursoy, N., Garrigue, J.S., Razafindratsita, A., Lambert, G., Benita, S., 2003. Excipient effects on in vitro cytotoxicity of a novel paclitaxel self-emulsifying drug delivery system. J. Pharm. Sci. 92 (12), 2411–2418.

Hampel, H., O'Bryant, S.E., Durrleman, S., Younesi, E., Rojkova, K., Escott-Price, V., Corvol, J.C., Broich, K., Dubois, B., Lista, S., 2017. A precision medicine initiative for Alzheimer's disease: the road ahead to biomarker-guided integrative disease modeling. Climacteric 20, 107–118.

He, C., Hu, Y., Yin, L., Tang, C., Yin, C., 2010. Effects of particle size and surface charge on cellular uptake and biodistribution of polymeric nanoparticles. Biomaterials 31 (13), 3657–3666.

Hong, M., Zhu, S., Jiang, Y., Tang, G., Pei, Y., 2009. Efficient tumor targeting of hydroxycamptothecin loaded PEGylated niosomes modified with transferrin. J. Control. Release 133, 96–102.

Ishak, R.A.H., Mostafa, N.M., Kamel, A.O., 2017. Stealth lipid polymer hybrid nanoparticles loaded with rutin for effective brain delivery – comparative study with the gold standard (Tween 80): optimization, characterization and Biodistribution. Drug Delivery 24 (1), 1874–1890.

Jankovic, J., Hunter, J.C., 2002. A double-blind, placebo-controlled and longitudinal study of riluzole in early Parkinson's disease. Parkinsonism Relat. Disord. 8, 271–276.

Johansson, D., Falk, A., Marcus, M.M., Svensson, T.H., 2012. Celecoxib enhances the effect of reboxetine and fluxetine on cortical noradrenaline and serotonin output in the rat. Prog. Neuropsychopharmacol. Biol. Psych. 39 (1), 143–148.

Josephine, L.J., Vijaya, C., Barnabas, W., 2014. Albumin nanoparticles coated with polysorbate 80 as a novel drug carrier for the delivery of antiretroviral drug-Efavirenz. Int J Pharm Investig 4 (3), 142–148.

Kaizaki, S., Tien, L.T., Pang, Y., Cai, Z., Tanaka, S., Numazawa, S., Bhatt, A.J., Fan, L.W., 2013. Celecoxib reduces brain dopaminergic neuronal dysfunction and improves sensorimotor behavioral performance in neonatal rats exposed to systemic lipopolysaccharide. J. Neuroinflam. 10, 45–59.

Khalil, N.M., Do Nascimento, T.C.F., Casa, D.M., Dalmolin, L.F., De Mattos, A.C., Hoss, I., Romano, M.A., Mainardes, R.M., 2013. Colloids Surf., B 101, 353–360.

Kim, H.W., Rapoport, S.I., Rao, J.S., 2011. Altered arachidonic acid cascade enzymes in postmortem brain from bipolar disorder patients. Mol. Psych. 16, 419–428.

Kreuter, J., 2012. Nanoparticulate systems for brain delivery of drugs. Adv. Drug Deliv. Rev. 64, 213–222.

Kumar, R., Yasir, M., Saraf, S.A., Gaur, P.K., Kumar, Y., Singh, A.P., 2013. Glyceryl monostearate based nanoparticles of mefenamic acid: fabrication and in vitro characterization. Drug Invention Today 5, 246–250.

Kyle, A.B., Laili, L., James, S., Murrough, W., 2013. Novel glutamatergic drugs for the treatment of mood disorders. Neuropsych. Dis. Treat. 9, 1101–1112.

Lau, C.G., Takeuchi, K., Rodenas-Ruano, A., Takayasu, Y., Murphy, J., Bennett, M.V., Zukin, R.S., 2009. Regulation of NMDA receptor Ca2+ signaling and synaptic plasticity. Biochem. Soc. Trans. 37, 1369–1374.

Leng, Y., Fessler, E.B., Chuang, D.M., 2013. Neuroprotective effects of the mood stabilizer lamotrigine against glutamate excitotoxicity: roles of chromatin remodeling and Bcl-2 induction. Int. J. Neuropsychopharm. 16, 607–620.

Li, J.O., Li, W.W., Jiang, Z.G., Ghanbari, H.A., 2013. Oxidative stress and neurodegenerative disorders. Int. J. Mol. Sci. 14 (12), 24438–24475.

Li, Y., Wong, H.L., Shuhendler, A.J., 2008. Molecular interactions, internal structure and drug release kinetics of rationally developed polymer–lipid hybrid nanoparticles. J. Control. Release 128, 60–70.

Lv, H., Zhang, S., Wang, B., Cui, S., Yan, J., 2006. Toxicity of cationic lipids and cationic polymers in gene delivery. J. Control. Release 114 (1), 100–109.

Martins, H.F., Pinto, D.P., Nascimento, V.A., Marques, M.A.S., Amendoeira, F.C., 2013. Determination of levodopa in human plasma by high performance liquid chromatography-Tandem mass spectroscopy (HPLC–MS/MS): application to a bioequivalence study. Quim. Nova 36 (1), 171–176.

Massaad, C.A., Klann, E., 2011. Reactive oxygen species in the regulation of synaptic plasticity and memory. Antioxid. Redox Signal. 14, 2013–2054.

Mayur, B., Zaved, A.K., 2015. Poly (n-butylcyanoacrylate) nanoparticles for oral delivery of quercetin: preparation, characterization, and pharmacokinetics and biodistribution studies in Wistar rats. Int. J. Nanomed. 10, 3921–3935.

Mcgeer, E.G., Mcgeer, P.L., 2007. The role of anti-inflammatory agents in Parkinson's disease. CNS Drugs 21, 789–797.

Modi, S., Swetha, M.G., Goswami, D., Gupta, G.D., Mayor, S., Krishnan, Y., 2009. A DNA nanomachine that maps spatial and temporal pH changes inside living cells. Nat. Nanotechnol. 4 (5), 325–330.

Moghimi, S.M., Szebeni, J., 2003. Stealth liposomes and long circulating nanoparticles: critical issues in pharmacokinetics, opsonization and protein-binding properties. Prog. Lipid Res. 42, 463–478.

Mustafa, G., Ahmad, N., Baboota, S., Alia, J., Ahuja, A., 2013. UHPLC/ESI-Q-TOF-MS method for the measurement of dopamine in rodent striatal tissue: a comparative effects of intranasal administration of ropinirole solution over nanoemulsions. Drug Test. Anal. 5 (8), 702–709.

Naeem, S., Ikram, R., Khan, S.S., Rao, S.S., 2017. NSAIDs ameliorate cognitive and motor impairment in a model of Parkinsonism induced by chlorpromazine. Pak. J. Pharm. Sci. 30 (3), 801–808.

Niehaus, W.G., Samuelson, B., 1968. Formation of malondialdehyde from phospholipids arachidonate during microsomal lipid peroxidation. Eur. J. Biochem. 6, 126–130.

Olanow, C.W., Stern, M.B., Sethi, K., 2009. The scientific and clinical basis for the treatment of Parkinson disease. Neurology 72, S1–S136.

Panayiotopoulos, C.P. (Ed.), A Clinical Guide to Epileptic Syndromes and their Treatment. Springer Healthcare, United Kingdom, 2010, pp. 173–235..

Papazisis, G., Kallaras, K., Kaiki-Astara, A., Pourzitaki, Ch., Tzachanis, D., Dagklis, Th., Kouvelas, D., 2008. Neuroprotection by lamotrigine in a rat model of neonatal hypoxic-ischaemic encephalopathy. Int. J. Neuropsychopharm. 11, 321–329.

Perrault, S.D., Walkey, C., Jennings, T., Fischer, H.C., Chan, W.C., 2009. Mediating tumor targeting efficiency of nanoparticles though design. Nano Lett. 9 (5), 1909–1915.

Porras, G., De Dedeurwaerdere, P., Li, Q., Marti, M., Morgenstern, R., Soh, R., Bezard, E., Morari, M., Meissner, W.G., 2014. L-Dopa-induced dyskinesia: beyond an excessive dopamine tone in the striatum. Sci. Rep. 4, 3730. https://doi.org/10.1038/srep03730.

Radenovic, L., Selakovic, V., Janac, B., Todorovic, D., 2007. Effect of glutamate antagonists on nitric oxide production in rat brain following intrahippocampal injection. Arch. Biol. Sci. 59 (1), 29–36. Retraction of: Radenovic L, Selakovic V, Janac B, Todorovic D. Arch Biol Sci Belgrade 2015; 67(2): 745.

Ramadan, E., Basselin, M., Rao, J.S., Chang, L., Chen, M., Ma, K., Rapoport, S.I., 2012. Lamotrigine blocks NMDA receptor-initiated arachidonic acid signaling in rat brain: Implications for its efficacy in bipolar disorder. Int. J. Neuropsychopharmacol. 15 (7), 931–943.

Roudier, B., Davit, B.M., Beyssac, E., Cardot, J.M., 2014. In vitro-in vivo correlation's dissolution limits setting. Pharm. Res. 31, 2529–2538.

Sallustio, B.C., Morris, R.G., 1997. High-performance liquid chromatography quantitation of plasma lamotrigine concentrations: application measuring trough concentrations in patients with epilepsy. Ther. Drug Monit. 19, 688–693.

Salvador-Morales, C., Zhang, L., Langer, R., Farokhzad, O.C., 2009. Immunocompatibility properties of lipid-polymer hybrid nanoparticles with heterogeneous surface functional groups. Biomaterials 30 (12), 2231–2240.

Sanberg, P.R., Giordano, M., Bunsey, M.D., Norman, A.B., 1988. The catalepsy test: its ups and downs. Behav. Neurosci. 102 (5), 748–759.

Sandhu, K., Rana, A., 2013. Evaluation of antiparkinson's activity of Nigella Sativa seeds in chlorpromazine induced experimental animal model. Academic Sciences 5 (3), 0975–1491.

Schapira, A.H., 2009. Molecular and clinical pathways to neuroprotection of dopaminergic drugs in Parkinson disease. Neurology 72, S44–S50.

Schwartz, M., Shechter, R., 2010. Systemic inflammatory cells fight off neurodegenerative disease. Nat. Rev. Neurol. 6, 405–410.

Senek, M., Nyholm, D., 2014. Continuous drug delivery in Parkinson's disease. CNS Drugs 28, 19–27.

Sestakova, N., Puzserova, A., Kluknavsky, M., Bernatova, I., 2013. Determination of motor activity and anxietyrelated behaviour in rodents: methodological aspects and role of nitric oxide. Interdiscipl. Toxicol. 6 (3), 126–135.

Sharma, N., Rana, A.C., Bafna, P., 2011. Effect of aqueous extract of Cynodon dactylon on reserpine induced catalepsy. Int. J. Pharm. Sci. 3 (4), 424–426.

Sheng, Y., Chang, L., Kuang, T., Hu, J., 2016. PEG/heparin-decorated lipid-polymer hybrid nanoparticles for long circulating drug delivery. RSC Adv. 6, 23279–23287.

Shin, H.W., Chung, S.J., 2012. Drug-induced Parkinsonism. J Clin Neurol 8 (1), 15–21.

Sinha, K.A., 1972. Colorimetric assay of catalase. Anal. Biochem. 47, 389–394.

Song, Z., Feng, R., Sun, M., Guo, C., Gao, Y., Li, L., Zhai, G., 2011. Curcumin-loaded PLGA-PEG-PLGA triblock copolymeric micelles: preparation, pharmacokinetics and distribution in vivo. J. Colloid Interface Sci. 354, 116–123.

Stanley, B.A., Sivakumaran, V., Shi, S., McDonald, I., Lloyd, D., Watson, W.H., Aon, M. A., Paolocci, N., 2011. Thioredoxin reductase-2 is essential for keeping low levels of H_2O_2 emission from isolated heart mitochondria. J. Biol. Chem. 286, 33669–33677.

Sun, S., Xie, C., Wang, H., Hu, Y., 2004. Specific role of polysorbate 80 coating on the targeting of nanoparticles to the brain. Biomaterials 25 (15), 3065–3071.

Takahashi, E., Niimi, K., Itakura, C., 2009. Motor coordination impairment in aged heterozygous rolling Nagoya, Cav2.1 mutant mice. Brain Res. 1279, 50–57.

Teismann, P., Ferger, B., 2001. Inhibition of the cyclooxygenase isoenzymes COX-1 and COX-2 provide neuroprotection in the MPTP-mouse model of Parkinson's disease. Synapse 39, 167–174.

Thevenot, J., Troutier, A.L., David, L., Delair, T., Ladaviere, C., 2007. Steric stabilization of lipid/polymer particle assemblies by poly (ethylene glycol)-lipids. Biomacromolecules 8, 3651–3660.

Vadlamudi, H.C., Yalavarthi, P.R., Venkata, B.R.M., Thanniru, J., Vandana, K.R., Sundaresan, C.R., 2016. Potential of microemulsified entacapone drug delivery systems in the management of acute Parkinson's disease. J Acute Dis 5 (4), 315–325.

Valencia, P.M., Basto, P.A., Zhang, L.F., Rhee, M., Langer, R., Farokhzad, O.C., Karnik, R., 2010. Single-step assembly of homogenous lipid-polymeric and lipid-quantum dot nanoparticles enabled by microfluidic rapid mixing. ACS Nano 4 (3), 1671–1679.

Valko, M., Leibfritz, D., Moncol, J., Cronin, M.T., Mazur, M., Telser, J., 2007. Free radicals and antioxidants in normal physiological functions and human disease. Int. J. Biochem. Cell Biol. 39, 44–84.

Varoglu, A.O., Yildirim, A., Aygul, R., Gundogdu, O.L., Sahin, Y.N., 2010. Effects of valproate, carbamazepine and levetiracetam on the antioxidant and oxidant systems in epileptic patients and their clinical importance. Clin. Nuropharmacol. 33, 155–157.

Vega-Avila, E., Pugsley, M.K., 2011. An overview of colorimetric assay methods used to assess survival or proliferation of mammalian cells. Proc. West. Pharmacol. Soc. 54, 10–14.

Vorhees, C.V., Williams, M.T., 2006. Morris water maze: procedures for assessing spatial and related forms of learning and memory. Nat. Protoc. 1 (2), 848–858.

Wang, H., Jia, Y., Hu, W., Jiang, H., Zhang, J., Zhang, L., 2013. Effect of preparation conditions on the size and encapsulation properties of mPEG-PLGA nanoparticles simultaneously loaded with vincristine sulfate and curcumin. Pharm. Dev. Technol. 18 (3), 694–1670.

Wilson, B., Samanta, M.K., Santhi, K., Kumar, K.P., Paramakrishnan, N., Suresh, B., 2008. Poly (n-butylcyanoacrylate) nanoparticles coated with polysorbate 80 for the targeted delivery of rivastigmine into the brain to treat Alzheimer's disease. Brain Res. 1200, 159–168.

Wong, H.L., Bendayan, R., Rauth, A.M., Wu, X.Y., 2006. Simultaneous delivery of doxorubicin and GG918 (Elacridar) by new polymer-lipid hybrid nanoparticles (PLN) for enhanced treatment of multidrug-resistant breast cancer. J. Control. Release 116, 275–284.

Yan, X.Q., Shi, Y.L., Jiang, Q.F., et al., 2017. Design of amphiphilic PCL-PEG-PCL block copolymers as vehicles of Ginkgolide B and their brain-targeting studies. J. Biomater. Sci. Polym. Ed. 28, 1497–1510.

Yuba, E., Kojima, C., Harada, A., Tana, Watarai S, Kono, K., 2010. pH-sensitive fusogenic polymer-modified liposomes as a carrier of antigenic proteins for activation of cellular immunity. Biomaterials 31 (5), 943–951.

Zhang, L., Zhang, L., 2010. Lipid-polymer hybrid nanoparticles: synthesis, characterization and applications. Nano Life 1, 163–173.

Zhang, L., Radovic-Moreno, A.F., Alexis, F., Gu, F.X., Basto, P.A., Bagalkot, V., Jon, S., Langer, R.S., Farokhzad, O.C., 2007. Co-delivery of hydrophobic and hydrophilic drugs from nanoparticle-aptamer bioconjugates. Chem. Med. Chem. 2, 1268–1271.

Zhang, L., Chan, J.M., Gu, F.X., Rhee, J.-W., Wang, A.Z., Radovic-Moreno, A.F., Alexis, F., Langer, R., Farokhzad, O.C., 2008. Self-assembled lipid-polymer hybrid nanoparticles: a robust drug delivery platform. ACS Nano 2 (8), 1696–1702.

Zhao, J., Chai, Y.D., Zhang, J., Huang, P.F., Nakashima, K., Gong, Y.K., 2015. Long circulating micelles of an amphiphilic random copolymer bearing cell outer membrane phosphorylcholine zwitterions. Acta Biomater. 16, 94–102.

Zheng, A., Kallio, A., Härkönen, P., 2007. Tamoxifen-induced rapid death of MCF-7 breast cancer cells is mediated via extracellularly signal-regulated kinase signaling and can be abrogated by estrogen. Endocrinology 148 (6), 2764–2777.